# \*Manuscript

**Click here to view linked References** 

- 1 Tropical Pacific Forcing of Late-Holocene Hydrologic Variability in the Coastal Southwest
- **2 United States**

3

- 4 Matthew E. Kirby<sup>1\*</sup>, Sarah J. Feakins<sup>2\*</sup>, Christine A. Hiner<sup>1</sup>, Joanna Fantozzi<sup>1</sup>, Susan R. H.
- 5 Zimmerman<sup>3</sup>, Theodore Dingemans<sup>4</sup>, Scott A. Mensing<sup>4</sup>
- 6 <sup>1</sup>California State University, Fullerton, Department of Geological Sciences, Fullerton, CA 92834 USA
- <sup>2</sup>University of Southern California, Department of Earth Sciences, Los Angeles, CA 90089 USA
- 8 Center for Accelerator Mass Spectrometry, Lawrence Livermore National Laboratory, Livermore CA 94550, USA
- 9 <sup>4</sup> Department of Geography, University of Nevada, Reno, NV 89557, USA
- 10 \*Corresponding authors: <a href="mkirby@fullerton.edu">mkirby@fullerton.edu</a>, <a href="feakins@usc.edu">feakins@usc.edu</a>

#### Abstract

12

13

14

15

16

17

18

19

20

21

22

23

24

25

26

27

28

29

30

31

32

Change in water availability is of great concern in the coastal southwest United States (CSWUS). Reconstructing the history of water pre-1800 AD requires the use of proxy data. Lakes provide long-lived, high-resolution terrestrial archives of past hydrologic change, and their sediments contain a variety of proxies. This study presents geochemical and sedimentological data from Zaca Lake, CA (Santa Barbara County) used to reconstruct a 3000 year history of winter season moisture source ( $\delta D_{wax}$ ) and catchment run-off (125–2000  $\mu m$  sand) at decadal resolution. Here we show that winter season moisture source and run-off are highly variable over the past 3000 years; superimposed are regime shifts between wetter or drier conditions that persist on average over multiple centuries. Moisture source and run-off do not consistently covary indicating multiple atmospheric circulation modes where wetter/drier conditions prevail. Grain-size analysis reveals two intervals of multi-century drought with less run-off that pre-datethe" epic droughts" asidentified by Cooketal. (2004). A well-defined wet period with more run-off is identified during the Little Ice Age. Notably, the grain size data show strong coherence with western North American percent drought area indices for the past 1000 years. As a result, our data extend the history of drought and pluvials back to 3000 calendar years BP in the <sub>CSW</sub>US. Comparison to tropical Pacific proxies confirms the long-term relationship between El Niño and enhanced run-off in the CSWUS. Our results demonstrate the long-term importance of the tropical Pacific to the <sub>CSW</sub>US winter season hydroclimate.

**Keywords:** climate; runoff; leaf wax; hydrogen isotope; drought

## 1. Introduction and Background

33

34

35

36

37

38

39

40

41

42

43

44

45

46

47

48

49

50

51

52

53

54

California is enduring extreme drought conditions during 2013–2014. Although the hydroclimate of the semi-arid region is inherently variable, with large interannual variability in precipitation (Dettinger et al., 1998), there is considerable concern that the recent dry years may be part of a drying trend (Williams et al., 2013). For the coastal southwest United States (CSWUS), future projections are for drier conditions with less frequent, but more intense precipitation (e.g., more atmospheric river events) and subsequent flood events (Das et al., 2013; Dettinger, 2011; Neelin et al., 2013; Pierce et al., 2013; Seager et al., 2013). This combination of hydroclimatic change represents a formidable challenge to the water resource and management infrastructure as well as to the ecology of the region (Loarie et al., 2008; Tanaka et al., 2006; Williams et al., 2013). Understanding past hydroclimatic variability and its forcings provides a baseline understanding of the dynamics that drive the hydroclimatic system. This baseline is important for examining present change and assessing future predictions. Today, the <sub>CSW</sub>US has an almost exclusively winter-season precipitation regime. Interannual variations in precipitation amount vary with the position of winter season storm tracks influenced by Pacific sea surface temperature (SST) patterns (Fig. 1) (Cook et al., 2011; Gan and Wu, 2013; Graham et al., 2007; Herweijer et al., 2006; Namias et al., 1988; Seager et al., 2005a) Variations in Pacific Ocean SSTs, including those associated with El Niño-Southern Oscillation (ENSO) as well as extratropical conditions such as that in the Kuroshio Extension region (northwest Pacific), have been shown to play important roles in driving precipitation amount variability, including both droughts and pluvials, on interannual to multi-decadal timescales in the <sub>CSW</sub>US (Andrews et al.,

2004; Castello and Shelton, 2004; Cook et al., 2011; DeFlorio et al., 2013; McCabe-Glynn et al., 2013; Wang et al., 2013).

55

56

57

58

59

60

61

62

63

64

65

66

67

68

69

70

71

72

73

74

75

76

77

How the tropical Pacific will influence future hydroclimatic change in this region is of particular interest. Research indicates that the frequency and perhaps intensity of El Niño events may increase with projected future warming (Ashok et al., 2012; Cai et al., 2014; Santoso et al., 2013) ENSO plays a major role in modern winter climatology of the <sub>CSW</sub>US (Castello and Shelton, 2004; Hanson et al., 2006; Schonher and Nicholson, 1989; Seager et al., 2005a). During the instrumental era, El Niño events are correlated with wetter than normal conditions in the CSWUS, which can produce extreme precipitation events and subsequent flooding (Cayan et al., 1999; Dettinger, 2011; Fye et al., 2004; Seager et al., 2005a); La Niña conditions are associated with drier than normal conditions (Castello and Shelton, 2004; Graham et al., 2007; Herweijer et al., 2006; Seager et al., 2005a). Paleoclimatic reconstructions can test the long-term relationship between ENSO and winter precipitation variability. Moreover, because winter season precipitation is the only significant contributor to the region's hydrologic budget, potential to study this unimodal climate regime without the noise associated with multi-season precipitation (e.g., in monsoon influenced areas). Finding long-lived, high-resolution terrestrial archives from the <sub>CSW</sub>US is a challenge. Most hydroclimatic reconstructions spanning the past 3,000 years from the <sub>CSW</sub>US are limited to multi-decadal to centennial scale resolution at best (Bird et al., 2010; Davis, 1992; Kirby et al., 2010; Kirby et al., 2004; Kirby et al., 2012). Tree ring networks provide a millennial view of variability particularly sensitive to drought conditions (Herweijer et al., 2007); however, they are less useful for reconstructing pluvials, nor does the tree ring network fully resolve spatial patterns across the <sub>CSW</sub>US, missing lowland areas below the tree-line (Macdonald and Case, 2005; Meko et al., 1980).

Here, we present sedimentological and geochemical results from Zaca Lake, CA to reconstruct hydroclimatic variability over the past 3,000 calendar years (cal yrs BP) at ~decadal resolution. This site fills an important geographical gap in knowledge representing the  $_{CSW}US$  region with large population centers and scarce water resources. We use leaf wax hydrogen isotopes ( $\delta D_{wax}$ ) and grain size (125–2000  $\mu m$  sand) to infer changes in moisture source and runoff, respectively. Regime shift analysis is applied to variable proxy records to statistically discern shifts in the mean state and to assess the coupling between moisture source and precipitation amount through time. Hydroclimatic proxies from Zaca Lake are compared to ENSO-related proxies to evaluate the role of the tropical Pacific on late-Holocene hydrologic variability in the coastal southwest United States.

## 2. Study Site and Methods

2.1 Study Site

88

89

90

91

92

93

94

95

96

97

98

99

100

101

102

103

104

105

106

107

108

109

2.2 Age Control and Sediment Analyses

Zaca Lake is a closed lake (0.08 km<sup>2</sup> lake area, 12 m water depth in July 2009) contained within a small (9 km<sup>2</sup>), steep sided catchment (730–1320 masl) (Feakins et al., 2014; Norris and Norris, 1994; Fig. 2). The lake has a spill-over elevation approximately 9 m above present lake level to a second basin, Overflow Lake, which is currently dry. Zaca Lake sediments extend deeper than the present core based on seismic profiling (Kirby and Simms, unpublished data). Sedimentation history in the adjacent Overflow Lake basin has been dated to 7,500 cal yrs BP with a charcoal sample from 450 cm depth (Padilla, 2010). The lake sits within the highly fractured and steeply dipping Monterey Formation. Consequently, a strong geomorphic contrast exists between the highly dissected, less vegetated south facing slopes and the more vegetated, less dissected north facing slopes (Fig. 2). There is also evidence for relict mass movement in the form of slumps and landslides as well as events documented within the historical record (Norris and Norris, 1994). Zaca Lake is a eutrophic, oligomictic lake with spring/summer CaCO<sub>3</sub> whiting events (Dickman, 1987; Sarnelle, 1992). Multi-month stratification produces hypolimnion anoxia and the build-up of H<sub>2</sub>S, occasionally causing fish mortality during turnover (Sarnelle, 1992). The hydrologic balance of the lake depends on direct precipitation, evaporation, overland flow, and groundwater contributions from an up-valley spring (Feakins et al., 2014; Ibarra et al., 2014). In the late 19<sup>th</sup> Century (Libeus family homestead est. 1891 AD), before significant human modification, lake levels were observed to fluctuate approximately 0.5–1.0 m on a seasonal basis (Norris and Norris, 1994).

Zaca Lake sediment core USC–ZACA09–1C (Z–1C) was obtained using a modified Livingston square rod piston corer. An intact sediment-water interface was collected on the first drive. The core was split, described, digitally photographed, and sub-sampled in the CSUF Paleoclimatology and Paleotsunami Laboratory. An overlapping core (Z–1D) was also obtained to confirm basin versus local sediment signals. The two cores have almost identical sedimentology. Seismic reflection data confirm that the core was extracted from a basin wide sediment unit (Kirby and Simms, unpublished data). All data presented in this paper come from the master core, Z–1C.

A combination of radiocarbon dating (n = 21) and reference horizon methods (n = 4) were used for age control. Discrete organic terrestrial macrofossils were picked under a binocular scope after wet sieving at 74 µm with deionized water (Table 1). Macrofossils were cleaned with standard acid-base-acid treatment and measured by Accelerator Mass Spectrometry (AMS) at the Lawrence Livermore National Laboratory. To build the chronology for the most recent sediments, we used the reference horizon method including the first appearance of non-native pollen types (*Eucalyptus* and *Erodium*), the  $^{137}$ Cs peak, and the intact sediment-water interface.

Mass magnetic susceptibility, loss-on-ignition (LOI) 550°C (total organic matter %), and LOI 950°C (total carbonate %) were determined for samples collected at 1 cm contiguous intervals following the same protocol as Kirby et al. (2007).

 $C_{org}/N_{total}$  ratios were determined for every other sample, i.e. 2 cm resolution. For the calculation of  $C_{org}/N_{total}$  ratios, it has been shown that the acidification of bulk sediments can change the nitrogen content in an unpredictable way (Brodie et al., 2011). Therefore, every sample was split and analyzed both untreated as well as treated (i.e., acidified) with 1 N HCl.  $N_{total}$  and  $C_{total}$  were determined on the untreated sample, and the acidified sample was used to

determine  $C_{org}$ .  $C_{org}/N_{total}$  ratios were measured using a Costech 4010 Elemental Analyzer and calculated following McFadden et al. (2005).

Grain size was determined at 1 cm contiguous intervals. Sediments for grain size analysis were treated with 30–50 mL of 30 %  $\rm H_2O_2$  to remove organic matter, 10 mL 1 N HCl to remove carbonates, and 10 mL 1 N NaOH to remove biogenic silica. Grain size was measured on a Malvern Mastersizer 2000 laser diffraction grain size analyzer coupled to a Hydro 2000G large volumesampledispersionunit. Astandardwasrunregularlytoverifytheequipment's accuracy and repeatability (Kirby tuff standard 2: n = 7831, mean = 4.6  $\mu$ m,  $\sigma = 0.15 \mu$ m). The 125–2000  $\mu$ m sand sized fraction is reported raw and smoothed with a 9-point moving average.

Charcoal was analyzed every 5 cm and at 1 cm across intervals of interest. Charcoal counts are based on the > 125  $\mu$ m size fraction using a modified LacCore methodology and calculated as the number of pieces counted per 1 g dry sediment weight (Whitlock and Larsen, 2001).

The hydrogen isotopic composition of the  $C_{28}$  *n*-alkanoic acids from plant leaf waxes were analyzed every 1 to 2 cm intervals (as reported in Feakins et al., 2014). Hydrogen isotopic (D/H) ratios are reported in standard  $\delta$ Dnotationinpermil(‰)units.

Regime shift analysis was performed on the sand % (after smoothing with a 9 point moving average to  $\sim 30$  yr resolution to reduce noise) and  $\delta D_{wax}$  values using the method of Rodionov (2004). The software parameters were set to identify p = < 0.05 significant changes in the mean value based on a two-tailedStudent'st -test. A 50-year cut-off length was prescribed withaHuber'sweightparameterof1.Norednoisewasincorporated.

2.3 Climatological Data

Zaca Creek monthly mean discharge data (m³ sec⁻¹) were obtained from the USGS

National Water Information System. Two sites, separated by 3.9 km distance, were used to
develop a complete record spanning 1941–2013 AD. Site one covered the period 1941–1963 AD

(25.9 km downstream from Zaca Lake) and Site 2 1963–2013 AD (22 km downstream from

Zaca Lake). This small difference in distance from source results in a change in the area drained
by 17 km² between Site 1 (102 km²) and Site 2 (85 km²). Despite this difference, the two records
are linked and interpreted as representative data for winter season (November to May) discharge
for the Zaca Lake drainage basin over the period 1941–2013 AD.

Winter precipitation data (November through March) were obtained from the Western Regional Climate Center NOAA Cooperative Stations for Southern California. Five sites spanning 1915 to 2010 AD were selected based on the completeness of data as well as their proximity to Zaca Lake (Fig. 1). These sites include: Los Alamos (1915 to 1998 AD), Cuyama (1943 to 1971 AD), Santa Barbara (1940 to 2010 AD), Lompoc (1949 to 2010 AD), and Santa Maria (1947 to 2010 AD). The data were averaged for the five sites and smoothed with a 5-point moving average to reduce inter-site noise. Although the absolute values vary from site to site, the direction of change is similar. We use these averaged data as a reliable measure of winter precipitation across the study region over the past 90 years.

#### 3. Results

172

173

174

175

176

177

178

179

180

181

182

183

184

185

186

187

188

189

190

191

192

193

194

3.1 Age Control

The sediments of Z–1C are dated with historical markers and AMS radiocarbon measurements on organic macrofossils. Starting at the top of the core, the modern sedimentwater interface was captured intact and defined as 2008 AD, the year of deposition prior to coring. The first appearance of *Erodium* pollen in the core was assigned an age of 1755–1760 AD based on timing of its appearance in the region (Mensing and Byrne, 1998). The first appearance of Eucalyptus was dated based on the time of planting and maturation and estimated at 1917 AD (Norris and Norris, 1994). The <sup>137</sup>Cs peak in the sediments was dated to the time of peak atmospheric concentrations in 1963 AD following nuclear weapons testing. Radiocarbon dates were obtained for a total of 21 organic macrofossil samples collected from the core (Table 1). <sup>14</sup>C dates were calibrated using the IntCal13 calibration curve (Reimer et al., 2009) with the Bacon v2.2 program (Blaauw and Christen, 2011). A Bayesian age model was constructed using the R-based statistical program Bacon v2.2 (Blaauw and Christen, 2011), based on 4 historical dates and 16 radiocarbon dates (Fig. 3). Overall, sedimentation rates average 0.3 cm yr<sup>-1</sup>. Of the 21 radiocarbon dates obtained, 16 are used for age control and 5 were excluded as discussed below. Two dates were discounted as they appear to represent incorporation of preaged material (by ca. 5000 and 1000 <sup>14</sup>C yrs; CAMS# 147070 and 147074 respectively); these outliers are not discussed further. In addition we discount three dates on very fine and delicate organic fragments from 778.5, 800.5, and 806.5 cm depths each yielding identical ages 100 <sup>14</sup>C yrs younger than the overlying date at 642 cm depth which shows no evidence of reworking (Table 1). This sequence of dates raises the question of instantaneous deposition of sediment from 808 to 648 cm in the core, for which we find no stratigraphic evidence briefly described as

follows. The base of the unit is not erosional and contains sub-cm scale laminae that are concordant across the basal section. The grain size data lack a sharp basal contact and indicate a gradual change in sediment texture across the base of the sediment unit. Geochemistry is inconsistent with a terrestrial input: we find low LOI 550°C, low  $C_{org}/N_{total}$ , low magnetic susceptibility, and low LOI 950°C. Each of these suggesting diminished terrestrial inputs including reduced transport of terrestrial organics and magnetic minerals into the lake. Analysis of littoral cores spanning the past 600 cal yrs BP indicate LOI 950°C values in excess of 70%, littered with abundant charaphytic stems and gastropod shells (Rubi, 2013). We find no evidence for this material having been transported in an event to the profundal zone. Finally, variable  $\delta D$  values suggest that leaf waxes were transferred into the lake over time, reflecting changes in water source. From these various structural and sedimentological data, we conclude that the three dates (778.5, 800.5 and 806.5 cm) are unreliable and thus are not included in the age model.

The core consists of sections of dark grey, black or brown alternating colored layers; light brownhomogenous units of varying thickness; occasional layers (1 -3 cm thick) of sandy silts or terrestrial organic material, including small twigs, grasses and charcoal; and, infrequent packets of carbonate laminae ( $\sim$ 1 mm) (Fig. 4). Based on whole core sedimentological averages, the lake is dominated by inorganic, non-carbonate clastic sedimentation (mean 81.0 %,  $\sigma$  = 12.7 %) with contributions from chemical and biogenic carbonates (mean = 9.3 %,  $\sigma$  = 11.0 %) and allochthonous and autochthonous organic matter (mean = 10.1 %,  $\sigma$  = 3.3 %).

Magnetic susceptibility, LOI 550°C, LOI 950°C,  $C_{org}/N_{total}$  ratios are characterized by large amplitude, multi-cm scale variability throughout the core, except between 2,700 and 2,000 cal yr BP where all of the above are uniformly low (Fig. 5).

The grain size data indicate the sediments are dominantly clayer silts with variable sand contributions. We find expected correlations between grain size categories (e.g., clay vs. sand, r = -0.78), and we focus on the sand sized fraction 125–2000 µm (hereafter "sand") for hydroclimatic interpretations as discussed in Section 4.1. In general, the grain size data are characterized by moderate amplitude, multi-cm scale variability throughout the core (Fig. 5). Using regime shift analysis on the 9-point averaged data we identify breakpoints demarcating intervals of lower and higher sand inputs. High input intervals are identified from 2790 -2520, 2000–1560,920–460(withanincreaseafter650), 370–240 and since 50 cal yrs BP (or 1900 AD, corresponding to most of the period of human occupation) (Fig. 6). Low input intervals include persistent lows between 2520–2000and 1560–920 as well as brief interludes from 460-370and240 -50 cal yrs BP (Fig. 6).  $\delta D_{\text{wax}}$  values range between -100 and -175 ‰, for the  $C_{28}$  *n*-alkanoic acid (Fig. 5). Details of molecular abundance distribution and isotopic composition of these results are provided by Feakins et al. (2014). Using regime shift analysis, we identified periods of on average more negative  $\delta D_{\text{wax}}$  values from 2690–1990 and since 990 cal yrs BP and more positive δD<sub>wax</sub> values between 3000–2690 and 1990–990 cal yrs BP, including a shift within this interval at 1420 cal yrs BP associated with one of the largest positive excursions of the entire record (Fig. 6).

218

219

220

221

222

223

224

225

226

227

228

229

230

231

232

233

234

235

#### 4. Discussion

237

238

239

240

241

242

243

244

245

246

247

248

249

250

251

252

253

254

255

256

257

258

259

4.1 Zaca Lake sand evidence for run-off

For hydroclimatic interpretations we focus on the sand record as a proxy for run-off, which has a demonstrable link to wet/dry climatic shifts in the region. Changes in sediment grain size in profundal lake sediments, particularly sand sized material, have often been interpreted in terms of run-off dynamics and/or climate wetness (Anderson, 2001; Conroy et al., 2008; Kirby et al., 2010; Sun et al., 2002). In the winter-dominated precipitation regime of coastal central and southern California, changes in river sediment load and flux show a positive correlation to climate wetness (Farnsworth and Milliman, 2003; Gray et al., 2014; Inman and Jenkins, 1999; Warrick and Mertes, 2009). Research on rivers that drain from the larger geographical region in which Zaca is located have shown that heavy rains, discharge and the mobilization of sand-sized sediments are associated with El Niño events in instrumental records between 1930 AD and 2000 AD (Gray et al., 2014). At Lake Elsinore, 275 km southeast of Zaca Lake, lake sediment grain size analysis reveals sand proportions rise with known 20<sup>th</sup> Century increases in the discharge of the San Jacinto River linked to the positive phase of the Pacific Decadal Oscillation (Kirby et al., 2010). Paleoclimatic reconstructions of wetness/run-off have been extended into the last glacial at Lake Elsinore and indicate wetter conditions during the last glacial from 19,000-12,600 cal yrs BP and comparatively drier conditions into the Holocene (~12,600 cal yrs BP) through modern, associated with higher and lower sand proportions, respectively (Kirby et al., 2010; Kirby et al., 2013). Zaca Lake has similar climatic, geomorphic, and limnologic conditions to Lake Elsinore; both are in a ~semi-arid environment with winter-dominated precipitation, a steep drainage basin and clastic-dominated sedimentation. As with Lake Elsinore, based on the precipitation-sediment

discharge studies discussed above, we interpret changes in the contribution of sand to the profundal zone of Zaca Lake over time as a proxy for run-off caused by changes in winter season precipitation. Because the bulk of the sand is in the very fine sand size fraction ( $\overline{}^{\square}$  = 89 % of total sand is between 62.5–124.99 µm), we use 125 to 2000 µm sand ( $\overline{}^{\square}$  = 10.7 % of total sand) as a conservative proxy of the requisite high energy run-off required to transport the larger sand size fractions. Because of this, our interpretation is likely skewed towards larger hydroclimatic changes; however, the omission of the very fine sand portion also reduces non-climatic noise associated with processes that mobilize smaller grain sizes (e.g., wave action winnowing and other resuspension processes).

To evaluate this proxy, we compare the 20<sup>th</sup> Century sand data to historical events documented from 1900 to 1993 AD at Zaca Lake including floods, fires, and observed lake status (Norris and Norris, 1994) (Fig. 7). Because these data are based on human memory and occasional diary/newspaper postings, they are possibly incomplete and subjective. We use also Google Earth historical imagery – although irregularly spaced – for the period between 1994 and 2010 AD. We use winter season monthly mean discharge from Zaca Creek to quantify run-off. Finally, we use a five-site winter season precipitation composite to examine precipitation variability since 1915 AD.

Within age model uncertainty, sand increases during documented lake highstands, floods, heavy precipitation events, and/or high Zaca Creek discharge years (Fig. 7). For example, the broad peak in sand between 1910 and 1923 AD is approximately coeval to noted highstands in both Zaca Lake and Overflow Lake as well as above average winter precipitation. This peak may correspond to the well-documented early 20<sup>th</sup> century pluvial (1905–1917 AD), known as possibly the wettest 13-year period in the past 1000 years in the western United States (Cook et

al., 2011). A peak in sand centered on 1935 AD follows a general increase in winter precipitation beginning in 1930 AD. A small peak in sand in 1943 AD is more likely associated with human disturbance (trail construction) in the drainage basin; although, there is a small peak in discharge centered on 1943 AD as well. Sand is high, but variable between 1948 and 1958 AD. This 10-year interval is associated with a period of intense construction and development in the lake's drainage basin; however, discharge and winter precipitation are generally below average. A small peak in sand ca. 1966 AD and a larger peak in 1972 AD are very close to peaks in discharge in 1967 AD and 1976 AD, respectively. The late 1990s show a strong relationship between run-off, lake status, winter precipitation amount, and sand. Finally, the largest sand peak occurs ca. 2004–2005 and is correlative with known highstands in both Zaca and Overflow Lake. In all, of the eight major increases in sand between 1900 and 2009 AD, six are most likely associated with documented hydrologic phenomena. Human disturbance is likely associated with two of the eight events (ca. 1943 and 1948 to 1958 AD).

Fire and its denudation of the landscape may also be important in preconditioning the landscape for run-off events (Lane et al., 2006; Reneau et al., 2007). For example there were major fires in the region in 1973 AD and 1996 AD. However, a comparison between sand and charcoal over the  $20^{th}$  Century reveals no consistent relationship (r = -0.09; p < 0.486) (Fig. 7); lagging the sand to the charcoal at 1 through 4 years made no difference in the relationship. Extending this comparison to the past 3,000 years also reveals no statistically significant relationship (r = 0.03; p < 0.608). Our observation may reflect the temporal difference in the response of sedimentation to fire versus its response to climatic affects. For example, fire is more comparable to a short-lived perturbation to alake scatch mentwith a strong immediate, but rapidly diminishing, response as vegetation recovers and stabilizes the hillslopes (Inbar et al.,

1998; Moody et al., 2013). Climatic change, on the other hand, generates decadal or longer preferred "states" such as pluvials or droughts (Fye et al., 2004; Cook et al., 2011). The impact of these long term changes in climate, especially in arid regions, on sedimentation is well documented: more precipitation = more run-off = more sediment transport (Farnsworth and Milliman, 2003; Gray et al., 2014; Inman and Jenkins, 1999; Warrick and Mertes, 2009). The latter studies illustrate the temporal differences between long-lived and persistent climate forced changes in run-off and short-lived fire-related perturbations. We conclude therefore that fire does not play a consistent or dominant role in explaining the sand-sized material transported into Zaca Lake at decadal to centennial timescales. Consequently, prior to significant human disturbance through construction (1900 AD), we interpret the sand proportion as primarily an indicator of precipitation driven run-off.

4.2 Zaca Lake hydrogen isotopic evidence for moisture source

Plant leaf wax hydrogen isotopic compositions ( $\delta D_{wax}$ ) are considered valuable archives of hydroclimatic information (Sachse et al., 2012). The plant leaf wax proxy records the  $\delta D$  of precipitation via a biological filter, which may modulate the nature of the recorded signal (Sachse et al., 2012).  $\delta D_{wax}$  values may be related to the  $\delta D$  values of precipitation ( $\delta D_{water}$ ) by an appropriate apparent fractionations ( $\epsilon_{wax/water}$ ):

Several of the dominant species in the catchment have been characterized in terms of the  $\delta D$  values of the n-alkanoic acids by Feakins et al. (2014), as well as the  $\delta D$  values of n-alkanes in multiple species from sites across California (Feakins and Sessions, 2010). Of these, *Quercus agrifolia*, co-dominant in the catchment today, is of most interest as the other co-dominant

species today, *Pinus coulteri* does not produce  $C_{28}$  *n*-alkanoic acids (Feakins et al., 2014). An  $\varepsilon_{\text{wax/w}}$  of –94‰(1compound  $\sigma$  =22‰, n = 10) has been determined from *Q. agrifolia* growing in the catchment today (Feakins et al., 2014). This provides the basis for interpreting  $\delta D_{\text{wax}}$  in terms of  $\delta D_{\text{water}}$ , yielding reasonable values from modern sediments (Feakins et al., 2014). However, we do not convert downcore measured values to precipitation isotope estimates given the potential for species change in the catchment (Dingemans et al., 2014), which may reasonably be expected to modulate catchment mean  $\varepsilon_{\text{wax/w}}$  over time (Feakins, 2013). We do however interpret relative shifts in  $\delta D_{\text{wax}}$  as a semi-quantitative proxy for shifts in precipitation isotopes.

Hydrogen isotopes in precipitation represent useful yet complex tracers of hydrological processes recording information about the history of a moisture parcel in terms of source region, storm track, condensation temperature, antecedent rainout, and finally post-condensation evaporation of the raindrop during descent (Buenning et al., 2013; Gat and Airey, 2006).

Downcore δD values are interpreted as principally responding to changes in moisture source region, with low δD values reflecting midlatitude N Pacific moisture sources (often associated with colder condensation temperatures and less post-condensation evaporation) and high δD values reflecting subtropical N Pacific moisture sources (often associated with warmer condensation temperatures and more post-condensation evaporation) (Buenning et al., 2013; Friedman et al., 2002; McCabe-Glynn et al., 2013). The only exception to this rule is that intense rainout in Atmospheric River events (AR; also known as "pineapple express type storms") can cause low δD values (Coplen et al., 2008) that may be indistinguishable from low δD values brought by intense storms originating from the midlatitude N Pacific (McCabe-Glynn et al., 2013). While these AR events do not dominate the storm tracks for the region, they do bring

disproportionate amounts of rainfall, perhaps 30–50% of precipitation in the region (Dettinger, 2013). Therefore low  $\delta D$  values are normally associated with intense precipitation whether from subtropical or midlatitude moisture sources, but low  $\delta D$  values can also be associated with modest precipitation totals from the midlatitude North Pacific, and vice versa for cold and wet conditions. In addition, wetter conditions, specifically with more antecedent rainout lead to more D-depleted precipitation, the "amount effect" (Lee and Fung, 2008); however, this is suggested to be a secondary isotope effect in observational and model studies of temporal variations in isotopes in this region (Buenning et al., 2013; McCabe-Glynn et al., 2013). High  $\delta D$  values are normally associated with weaker precipitation amounts from subtropical moisture sources as well as warm and dry conditions due to the temperature of condensation and post-condensation evaporative processes (Buenning et al., 2013). We therefore interpret changes in  $\partial D_{wax}$  with these observations in mind, i.e., that the primary isotope effects are expected to be associated with moisture source changes between subtropical and midlatitude N Pacific moisture source, but additional isotope effects may exert secondary controls. We view the 3,000 yr  $\delta D_{wax}$  record as a valuable temporal record of how precipitation isotopes may vary over time, but given that there is not a unique solution to explain  $\delta D_{precipitation}$  variations, we attempt to not oversimplify the possible interpretations of this complex hydrological tracer in our discussions of the climatic interpretations that follow.

### 4.2 Comparison of sand and leaf wax proxies

351

352

353

354

355

356

357

358

359

360

361

362

363

364

365

366

367

368

369

370

371

372

373

From the sediments of Zaca Lake we present two hydroclimatic proxies: we propose to track run-off using sand and precipitation moisture sources using  $\delta D_{wax}$  (Fig. 6). Both proxies relate exclusively to the winter-season. The unimodal precipitation regime generates run-off almost exclusively in winter. Likewise studies of plant water uptake suggest that plants are

recording the isotopic composition of winter-season precipitation, with no recorded signal during the summer dry season (Feakins and Sessions, 2010; Tipple et al., 2013). Because both analyses are determined on the same sediment core, we have a unique opportunity to directly compare two hydroclimatic proxies (Fig. 6). Intriguingly, we find no significant correlation between  $\partial D_{wax}$  and sand. Furthermore, while some regime shifts are concordant, many are not (Fig. 6). Our data therefore eschews a simple linkage of wetter conditions (high run-off) with any particular atmospheric circulation (as recorded by  $\partial D_{wax}$ ) and instead it appears that wetter winters can be created either with enhanced moisture delivery from midlatitude (more D-depleted) or subtropical N Pacific (usually, but not always, less D-depleted) moisture sources. However, while both proxies have uncertainties as quantitative proxies of hydrological conditions we have reason to believe that both carry important hydroclimatic information. We therefore consider the details of the record across the last 3,000 cal yrs BP to see what complementary information can be extracted from evaluation of both proxies (Fig. 6).

4.3 Hydroclimate reconstructions spanning 3,000 years

We begin with the highest (pre-settlement) sand proportions from 370–240 cal yrs BP, which we infer to be the wettest interval of the past 3000 years at Zaca Lake. We find an earlier high pulse from 500–450 cal yrs BP. Together, these two pulses, overlap with the Little Ice Age (LIA), a time of generally cold and wet conditions around the North Atlantic and perhaps throughout the Northern Hemisphere (Larsen et al., 2013; Mann et al., 2009). Stocker (2013) identifies the span of the LIA as 500–100 cal yrs BP, and it is also known to have multiple pulses from glacier advance records (Larsen et al., 2013; Schimmelpfennig et al., 2012). Peak run-off from 370–240 cal yrs BP is also associated with an abrupt decrease in δD<sub>wax</sub> data, suggesting a rapid shift to more N Pacific sourced moisture and/or a more significant "amounteffect"

associated with higher intensity storms. This century long shift in  $\delta D_{wax}$  data is not detected as a regime break by our methods, but falls within a 1000 yr regime with more D-depleted precipitation on average. The timing of this peak wet climate at Zaca Lake is approximately coeval to peak wet conditions at Lake Elsinore (350–265 cal yrs BP), located 275 km south of Zaca Lake (Kirby et al., 2010). We note also an abrupt drying at the end of the wet event as recorded at both Zaca Lake and Lake Elsinore.

397

398

399

400

401

402

403

404

405

406

407

408

409

410

411

412

413

414

415

416

417

418

419

Our data also identifies a dry interval between 1560 and 900 cal yrs BP, followed by moderately dry oscillating conditions until 650 cal yrs BP, overlapping with the timing of the MCA (1050–600 cal yrs BP; Fig. 6; (Stocker, 2013)). Some of these droughts may correspond to the "epicdroughts" identified between 650–1050 cal yrs BP (Cook et al., 2004) from the tree ring records across the southwest (Fig. 8). Multi-proxy comparison here reveals that the multicentennial scale dry period from 1560 and 920 cal yrs BP is associated with a high  $\delta D_{\text{wax}}$  regime from 1420 to 990 cal yrs BP, which suggests a dominantly subtropical moisture source. In particular, peak  $\delta D_{\text{wax}}$  values ca. 1400 cal yrs BP, as well as at 1300 and 1000 cal yrs BP, each corresponds to low run-off. Multi-century droughts from 900 to 600 cal yrs BP all have low  $\delta D_{\text{wax}}$  values suggesting a midlatitude N Pacific source and thus a different atmospheric cause for drought. These multi-decadal droughts correspond to the "epic" tree -ring droughts (Cook et al., 2004), in particular the severe drought of 1050 cal yrs BP (Fig. 8). However, we note that these droughts are not as persistent as the multi-centennial droughts deeper in the Zaca Lake sediments spanning 920–1560 cal yrs BP (interrupted by pluvials of <100yrs) and 2000–2500 cal yrs BP (uniformly dry) (Fig. 8).

The most extreme and persistent drought in the 3000 yr Zaca Lake record occurs between 2500 and 2000 cal yrs BP, following several hundred years of high run-off (Dingemans et al.,

2014). The Zaca Lake sand data are uniformly low between 2500 to 2000 cal yrs BP indicating limited run-off. The  $\delta D_{wax}$  indicate a systematic change in moisture source 200 years earlier (~2700 cal yrs BP) than the sand data. This persistent drought corresponds to a drought identified in the central Great Basin as period of aridity between 2800 and 1850 cal yrs BP and referred to as the Late-Holocene Dry Period (LHDP) by Mensing et al. (2013) (Fig. 6).  $\delta D_{wax}$  values average -154% during this time period. Based on  $\epsilon_{wax/w}$  of -94% (1compound  $\sigma$  =22%, n = 10) for Q. agrifolia (Feakins et al., 2014), we might infer precipitation isotopes during this time interval were around -73%, whichismoredepletedthanmodernvalues averaging ca. -50% (Feakins et al., 2014). Low  $\delta D$  values during warm and dry conditions suggest on average a more northerly Pacific moisture source than today. Intriguingly there are signs that this long drought coincided with less intense La Niña and El Niño conditions in the tropical Pacific (see Section 4.4), and this would be entirely consistent with the interpretation of low precipitation totals with a northerly moisture source for this multi-centennial drought.

In summary, the Zaca Lake record reveals several multi-centennial pluvials, including those associated with the widespread climatic anomaly at the time of the LIA, documenting the geographic spread of this event to include the <sub>CSW</sub>US. We provide compelling evidence for 2 droughts, lasting half a millennia each, within the last 3000 years. These severe, long-lasting droughts, beyond the extent of the tree ring reconstructions, add new information to the timing, duration and severity of multi-centennial droughts in the <sub>CSW</sub>US.

4.4 Tropical Pacific forcing of <sub>CSW</sub>US Winter hydroclimates over 3,000 years

It is well-known that Pacific Ocean SSTs play an important role in winter season hydroclimates along the <sub>CSW</sub>US at interannual to multi-decadal timescales (Herweijer et al., 2007; Namias et al., 1988; Ren et al., 2008; Seager et al., 2005b). Figure 1 illustrates this

relationship with a comparison of November to March (1949–2008 AD) surface precipitation rates (Hoerling et al., 2001) to tropical Pacific SST 1<sup>st</sup> EOF values (Kalnay et al., 1996). To assess this role in the past, we compare the Zaca Lake sand evidence for run-off to various lines of evidence from ENSO-related proxies. Zaca sand shows some coherent variations with sand evidence for run-off from the Galapagos Islands in the eastern equatorial Pacific (Conroy et al., 2008), demonstrating that precipitation and run-off amounts over the eastern equatorial Pacific (EEP) and over <sub>CSW</sub>US are linked (Fig. 9A and B). The two records are less similar between 600 and 100 cal yrs BP indicating a more complex response to the dynamics of the LIA and its respective forcings between the tropical Pacific and the <sub>CSW</sub>US. We also compare to molecular proxies for general (cholesterol) and specific (dinosterol) productivity changes from the Peruvian margin used to infer La Niña and El Niño activity, respectively (Makou et al., 2010) (Fig. 9C). This lower resolution record shows periods of higher ENSO variability (both La Niña and El Niño), which correspond to times of high sand run-off in both Galapagos and Zaca. However, between 3000 and 2100 cal yrs BP, the lower resolution cholesterol and dinosterol data (only 4 data points) make the comparison to Zaca less robust. Nonetheless, the cholesterol and dinosterol data during this interval are characterized by low values indicative of fewer intense La Niñas and El Niños (Makou et al., 2010) (Fig. 9C). There are no cholesterol and dinosterol data younger than 550 cal yrs BP for comparison to the Galapagos or Zaca.

443

444

445

446

447

448

449

450

451

452

453

454

455

456

457

458

459

460

461

462

463

464

465

Our comparison indicates that oceanic conditions in the tropical Pacific have played an important role in modulating winter season precipitation, and thus run-off, in the <sub>CSW</sub>US over the past 3000 years (Fig. 9). We find that evidence for more intense, or more frequent, El Niño corresponds with more run-off driven sand inputs into Zaca Lake across most of the past 3000 years. This new, well-dated record and coherent regional comparison supports the persistence of

the modern observations of ENSO controls on hydroclimate in the  $_{CSW}US$  (El Niño = more runoff).

Intriguingly, we do not find a predictable relationship between the  $\delta D_{wax}$  proxy for precipitation isotopes and ENSO-related records. While there are different modes of El Niño (Yu and Kim, 2013) it is perhaps surprising that there is not a consistent isotopic pattern associated with ENSO modulation of winter-season atmospheric circulation and precipitation in the  $_{CSW}US$ . If the leaf wax proxy record is a consistent recorder of precipitation isotopes in this lake then the  $\delta D_{wax}$  record implies multiple mean state differences of atmospheric circulation and moisture supply even during mean state shifts of ENSO. While much progress has been made in untangling the isotopic signatures of modern precipitation, we need more observational data of temporal variability in precipitation isotopes and isotope-enabled model experiments to better understand the processes that may lead to precipitation isotope variations associated with ENSO mean state changes, in order to fully access the diagnostic information embedded within these complex hydrological tracers.

### 5. Summary

We present a multi-proxy paleoclimatic record from Zaca Lake revealing a highly variable winter hydroclimate over the past 3000 years. Sand inputs record large amplitude variability in run-off in the Zaca catchment, with more sand associated with wetter conditions.

The LIA corresponds to byfarthewettestintervalinourrecordpeakingbetween370 —240 cal yrs BP. This event is coeval with a wet period identified in Lake Elsinore run-off (Kirby et al., 2010), indicating a coherent wet signal across CSWUS during the LIA. At the other extreme, low sand inputs into Zaca Lake from2570–2000 cal yrs BP, corroborates evidence for a sustained drought in the southwest, the LHDP (Mensing et al., 2013). TheLHDP's exceptionally long duration dwarfs the "epicdroughts" identified in the tree ringarchives from the interior southwest during the MCA (Cook et al., 2004). During the MCA we do find a series of multidecadal to centennial droughts recorded in Zaca Lake, interrupted by multi-decadal to centennial pluvials, however on average and in the extremes, conditions are not as severe as during the LHDP.

We also find large amplitude variability in plant leaf wax  $\delta D$ valuesrangingfrom -100% to-170% (Feakins et al., 2014). Leaf wax based precipitation reconstructions indicate regime shifts between preferred modes of atmospheric circulation tapping into midlatitude or subtropical N Pacific moisture across multi-centennial timescales. High frequency variability is apparent throughout the record sometimes between adjacent decadal samples and sometimes persisting for a century or more (e.g., peak LIA conditions) or longer shifts in mean conditions lasting up to a thousand years. The relationship between the  $\delta D_{wax}$  and sand provides robust evidence spanning 3 ka that the isotopic composition of precipitation is not straightforward indicator of the amount of precipitation in the region. Indeed the "amounteffect" has been shown to be at most a second-

order isotope effect in the region (Buenning et al., 2013). Instead precipitation isotopes have been shown to inform upon moisture source regions (Friedman et al., 2002; McCabe-Glynn et al., 2013). The Zaca Lake sand and  $\delta D$  proxy records therefore demonstrate that wet or dry conditions can be variably associated with subtropical or midlatitude N Pacific moisture sources. This multiproxy finding highlights the variable nature of moisture supply with storm tracks in the region, suggesting that isotopes provide a tracer of atmospheric processes that may be deconvolved to allow for mechanistic insights into atmospheric causes of droughts and pluvials. We find multiple atmospheric circulation modes where wetter/drier conditions prevail.

Regional comparisons of our 3000 yr hydroclimatic record support the hypothesis that tropical Pacific forcing is an important control on winter season hydroclimatology in the CSWUS. In general, El Niño-like conditions are associated with enhanced run-off in the Zaca catchment. The Zaca Lake sand record extends the instrumental record and documents the existence of an extreme pluvial during the LIA, which may be associated to warm EEP SSTs and an extended duration multi-centennial drought from 2570 to 2000 cal yrs BP, which may be associated with diminished ENSO (both La Niña and El Niño) variability and/or intensity. Hydrogen isotopes embedded in plant leaf waxes provide promising insights into atmospheric circulation changes. Further analysis of isotopic tracers may be able to reveal insights into how and why persistent drought conditions or intense pluvials can be created, to provide new predictive power that is neededtoaddressCalifornia'swaterchallengesahead.

## **Author Contributions**

Author contribution statement: MK and SF designed the study, collected the sediment cores and led the research. MK led the sedimentology and geochemistry; sampled the core; constructed the

526 age model and graphed the data and led the writing. SF led leaf wax hydrogen isotope 527 interpretations and contributed to the writing. CH and JF conducted all sedimentologic analyses. 528 SZ conducted radiocarbon measurements. TD and SM contributed to interpretations of the 529 climate record. All authors read and commented on the manuscript. 530 531 Acknowledgements 532 Funding for this project includes support from: NSF EAR-1002649 to SJF, MEK and 533 NSF EAR-0318511 to MEK. Funding for the radiocarbon dates was provided by LLNL grant 534 LDRD-09-ERI-003 to SRZ; this is LLNL-JRNL-653836. Thanks to Alex Simms (UCSB) for 535 help with the seismic reflection survey, Zaca Lake Retreat for access to the lake and their 536 hospitality, and Dr. Ken Adams and an anonymous reviewer for insightful and helpful reviews. 537 538 **Figure Captions** 539 Figure 1. Western United States showing correlation between November to March (1949–2008 AD) surface precipitation rates (Hoerling et al., 2001) to tropical Pacific SST 1<sup>st</sup> EOF (empirical 540 541 orthogonal function) values (Kalnay et al., 1996). Precipitation sites are numbered on figure: 1) 542 Los Alamos, 2) Lompoc, 3) Santa Maria, 4) Cuyama, 5) Santa Barbara. CA = California, NV = 543 Nevada, OR = Oregon, WA = Washington. 544 545 Figure 2. Map of Zaca Lake catchment. Inset map: bathymetry and location of core USC-546 ZACA09-1C.

Figure 3. Bayesian age model for USC-ZACA09-1C. Calibrated <sup>14</sup>C dates (blue), and first 548 occurrence of exotic pollen and <sup>137</sup>Cs peak (green), all with their 2-sigma error range. 549 550 551 Figure 4. Sediment core photographs for USC-ZACA09-1C. Color change between 673 and 552 688 cm is a photographic artifact. 553 554 Figure 5. USC-ZACA09-1C sedimentological and geochemical data. A) Magnetic susceptibility (x10<sup>-7</sup> m<sup>3</sup> kg<sup>-1</sup>). B) Percent loss on ignition 550°C (% total organic matter). C) 555 556 Percent loss on ignition 950°C (% total carbonate). D) Volume percent grain size (sand, silt, 557 clay). E) Percent sand >125 to 2000  $\mu$ m (thin line), 9-point smooth data (bold line). F)  $\delta D_{\text{wax}}$ values, C<sub>28</sub> *n*-alkanoicacid(‰) . G) C/N ratios. H) Charcoal counts. 558 559 560 Figure 6. USC-ZACA09-1C sedimentological and geochemical data. A) 9-point smoothed sand 561 % (125–2000  $\mu$ m). The thin overlying line shows the p < 0.05 regime shifts (Rodionov, 2004). 562 B)  $\delta D_{\text{wax}}$  values(‰) (Feakins et al., 2014). The thin overlying line shows the p < 0.05 regime 563 shifts (Rodionov, 2004). Shading is based on sand regime shift data. Blue = more run-off, orange 564 = less run-off. Timing of LIA and MCA based on IPCC (2013). Timing for LHDP based on 565 Mensing et al. (2013). 566 Figure 7. 20<sup>th</sup> Century USC–ZACA09–1C sand and historical data comparison. A) Sand (%) 567 568 (125–2000 μm). 2003 AD sand peak at 24.7 % is cut-off at 15 % by the left y-axis. B) Zaca Creek winter (Nov-Mar) discharge (m<sup>3</sup> sec<sup>-1</sup>). No data before 1941 A.D. Missing data: 2007, 569 570 2004, 1993–1992, 1988–1981, C) Winter (Nov-Mar) 5-site averaged total winter precipitation

571 (cm). D) Charcoal counts. Red circles = documented fire in the Zaca Lake drainage basin; M = 572 documented mudflow. 573 574 Figure 8. USC-ZACA09-1C 9-point smoothed percent sand comparison (A) to Cook et al. 575 (2004) western North America drought percent (60–point smooth) (B). D/W = the four 576 driest/wettest epochs (p < 0.05, those with confident limits above/below the long term mean (text 577 taken from Cook et al., 2004; Figure 2)). 578 579 Figure 9. USC–ZACA09–1C sand comparison to various equatorial and north Pacific ENSO/ 580 SSTs indices. A) 9-point smoothed sand % (125–2000  $\mu$ m). The thin overlying line shows the p 581 < 0.05 regime shifts (Rodionov, 2004). B) Sand-El Niño proxy from the Galapagos Islands 582 (Conroy et al., 2008). C) Molecular organic geochemistry proxy from the Peruvian margin used 583 to infer El Niño and La Niña intensity/activity (Makou et al., 2010). Shading is based on sand 584 regime shift data. Blue = more run-off, orange = less run-off. Boxes demarcate span of LIA and MCA (IPCC, 2014) and Late-Holocene Dry Period (LHDP) (Mensing et al., 2013). F = flood 585 586 layers identified in Santa Barbara Basin sediment cores over the past 2,000 cy BP (Hendy et al., 587 2013; Schimmelmann et al., 2003).

- 589 References
- Anderson, R.Y., 2001. Rapid changes in Late Pleistocene precipitation and stream discharge
- determined from medium- and coarse-grained sediment in saline lakes. Global and Planetary
- 592 Change 28, 73-83.
- Andrews, E.D., Antweiler, R.C., Neiman, P.J., Ralph, F.M., 2004. Influence of ENSO on Flood
- 594 Frequency along the California Coast. Journal of Climate 17, 337-348.
- Ashok, K., Sabin, T.P., Swapna, P., Murtugudde, R.G., 2012. Is a global warming signature
- emerging in the tropical Pacific? Geophysical Research Letters 39, L02701.
- 597 Bird, B.W., Kirby, M.E., Howat, I.M., Tulaczyk, S., 2010. Geophysical evidence for Holocene
- lake-level change in southern California (Dry Lake). Boreas 39, 131-144.
- Blaauw, M., Christen, J.A., 2011. Flexible paleoclimate age-depth models using an
- autoregressive gamma process. 457-474.
- Brodie, C.R., Leng, M.J., Casford, J.S.L., Kendrick, C.P., Lloyd, J.M., Yongqiang, Z., Bird,
- 602 M.I., 2011.EvidenceforbiasinCandNconcentrations δ13Ccompositionofterrestrial and
- aquatic organic materials due to pre-analysis acid preparation methods. Chemical Geology 282,
- 604 67-83.
- Buenning, N.H., Stott, L., Kanner, L., Yoshimura, K., 2013. Diagnosing Atmospheric Influences
- on the Interannual 18 O/16 O Variations in Western US Precipitation. Water (20734441) 5.
- 607 Cai, W., Borlace, S., Lengaigne, M., van Rensch, P., Collins, M., Vecchi, G., Timmermann, A.,
- Santoso, A., McPhaden, M.J., Wu, L., England, M.H., Wang, G., Guilyardi, E., Jin, F.-F., 2014.
- Increasing frequency of extreme El Nino events due to greenhouse warming. Nature Clim.
- 610 Change 4, 111-116.

- 611 Castello, A.F., Shelton, M.L., 2004. Winter precipitation on the US Pacific coast and El Nino-
- 612 Southern Oscillation events. International Journal of Climatology 24, 481-497.
- 613 Cayan, D.R., Redmond, K.T., Riddle, R.G., 1999. ENSO and hydrologic extremes in the western
- United States. Journal of Climate 12, 2881-2893.
- 615 Conroy, J.L., Overpeck, J.T., Cole, J.E., Shanahan, T.M., Steinitz-Kannan, M., 2008. Holocene
- changes in eastern tropical Pacific climate inferred from a Galapagos lake sediment record.
- Quaternary Science Reviews 27, 1166-1180.
- 618 Cook, B.I., Seager, R., Miller, R.L., 2011. On the Causes and Dynamics of the Early Twentieth-
- 619 Century North American Pluvial\*. Journal of Climate 24, 5043-5060.
- 620 Cook, E.R., Stahle, D.W., Woodhouse, C.A., Eakin, C.M., Meko, D.H., 2004. Long-term aridity
- changes in the western United States. Science 306, 1015-1018.
- 622 Coplen, T.B., Neiman, P.J., White, A.B., Landwehr, J.M., Ralph, F.M., Dettinger, M.D., 2008.
- Extreme changes in stable hydrogen isotopes and precipitation characteristics in a landfalling
- 624 Pacific storm. Geophysical Research Letters 35.
- Das, T., Maurer, E.P., Pierce, D.W., Dettinger, M.D., Cayan, D.R., 2013. Increases in flood
- magnitudes in California under warming climates. Journal of Hydrology 501, 101-110.
- Davis, O.K., 1992. Rapid climatic change in coastal southern California inferred from pollen
- analysis of San Joaquin Marsh. Quaternary Research 37, 89-100.
- 629 DeFlorio, M.J., Pierce, D.W., Cayan, D.R., Miller, A.J., 2013. Western U.S. Extreme
- 630 Precipitation Events and Their Relation to ENSO and PDO in CCSM4. Journal of Climate 26,
- 631 4231-4243.

- 632 Dettinger, M., 2011. Climate Change, Atmospheric Rivers, and Floods in California A
- Multimodel Analysis of Storm Frequency and Magnitude Changes 1. JAWRA Journal of the
- American Water Resources Association 47, 514-523.
- Dettinger, M.D., 2013. Atmospheric Rivers as Drought Busters on the US West Coast. Journal of
- Hydrometeorology 14.
- Dettinger, M.D., Cayan, D.R., Diaz, H.F., Meko, D.M., 1998. North-South precipitation patterns
- in western North America on interannual-to-decadal timescales. Journal of Climate 11, 3095-
- 639 3111.
- Dickman, M., 1987. Lake sediment microlaminae and annual mortalities of photosynthetic
- bacteria in an oligomictic lake. Freshwater Biology 18, 151-164.
- Farnsworth, K.L., Milliman, J.D., 2003. Effects of climatic and anthropogenic change on small
- 643 mountainous rivers: the Salinas River example. Global and Planetary Change 39, 53-64.
- 644 Feakins, S.J., 2013. Pollen-corrected leaf wax D/H reconstructions of northeast African
- 645 hydrological changes during the late Miocene. Palaeogeography, Palaeoclimatology,
- 646 Palaeoecology 374, 62-71.
- 647 Feakins, S.J., Kirby, M.E., Cheetham, M.I., Ibarra, Y., Zimmerman, S.R., 2014. Fluctuation in
- leaf wax D/H ratio from a southern California lake records significant variability in isotopes in
- precipitation during the late Holocene. Organic Geochemistry 66, 48-59.
- 650 Feakins, S.J., Sessions, A.L., 2010. Controls on the D/H ratios of plant leaf waxes in an arid
- ecosystem. Geochimica et Cosmochimica Acta 74, 2128-2141.
- 652 Friedman, I., Harris, J.M., Smith, G.I., Johnson, C.A., 2002. Stable isotope composition of
- waters in the Great Basin, United States 1. Air-mass trajectories. J. Geophys. Res. 107, 4400.

- 654 Fye, F.K., Stahle, D.W., Cook, E.R., 2004. Twentieth-Century Sea Surface Temperature Patterns
- in the Pacific during Decadal Moisture Regimes over the United States\*. Earth Interactions 8, 1-
- 656 22.
- 657 Gan, B., Wu, L., 2013. Seasonal and Long-Term Coupling between Wintertime Storm Tracks
- and Sea Surface Temperature in the North Pacific. Journal of Climate 26, 6123-6136.
- 659 Gat, J.R., Airey, P.L., 2006. Stable water isotopes in the atmosphere/biosphere/lithosphere
- interface: Scaling-up from the local to continental scale, under humid and dry conditions. Global
- and Planetary Change 51, 25-33.
- Graham, N.E., Hughes, M.K., Ammann, C.M., Cobb, K.M., Hoerling, M.P., Kennett, D.J.,
- Kennett, J.P., Rein, B., Stott, L., Wigand, P.E., 2007. Tropical Pacific-mid-latitude
- teleconnections in medieval times. Climatic Change 83, 241-285.
- 665 Gray, A.B., Warrick, J.A., Pasternack, G.B., Watson, E.B., Goñi, M.A., 2014. Suspended
- sediment behavior in a coastal dry-summer subtropical catchment: effects of hydrologic
- preconditions. Geomorphology.
- Hanson, R., Dettinger, M., Newhouse, M., 2006. Relations between climatic variability and
- 669 hydrologic time series from four alluvial basins across the southwestern United States.
- 670 Hydrogeology Journal 14, 1122-1146.
- Hendy, I.L., Dunn, L., Schimmelmann, A., Pak, D.K., 2013. Resolving varve and radiocarbon
- chronology differences during the last 2000 years in the Santa Barbara Basin sedimentary record,
- 673 California. Quaternary International 310, 155-168.
- Herweijer, C., Seager, R., Cook, E.R., 2006. North American droughts of the mid to late
- 675 nineteenth century: a history, simulation and implication for Mediaeval drought. The Holocene
- 676 16, 159-171.

- Herweijer, C., Seager, R., Cook, E.R., Emile-Geay, J., 2007. North American Droughts of the
- Last Millennium from a Gridded Network of Tree-Ring Data. Journal of Climate 20, 1353-1376.
- 679 Ibarra, Y., Corsetti, F.A., Cheetham, M.I., Feakins, S.J., 2014. Were fossil spring-associated
- 680 carbonates near Zaca Lake, Santa Barbara, California deposited under an ambient or thermal
- 681 regime? Sediment. Geol. 301, 15-25.
- Inman, D.L., Jenkins, S.A., 1999. Climate change and the episodicity of sediment flux of small
- 683 California Rivers. Journal of Geology 107, 251-270.
- Kalnay, E., Kanamitsu, M., Kistler, R., Collins, W., Deaven, D., Gandin, L., Iredell, M., Saha,
- 685 S., White, G., Woollen, J., Zhu, Y., Chelliah, M., Ebisuzaki, W., Higgins, W., Janowiak, J., Mo,
- 686 K.C., Ropelewski, C., Wang, J., Leetmaa, A., Reynolds, R., Jenne, R., Joseph, D., 1996. The
- NCEP/NCAR 40-year reanalysis project. Bulletin American Meteorological Society 77, 437-
- 688 471.
- Kirby, M., Lund, S., Patterson, W., Anderson, M., Bird, B., Ivanovici, L., Monarrez, P., Nielsen,
- 690 S., 2010. A Holocene record of Pacific Decadal Oscillation (PDO)-related hydrologic variability
- in Southern California (Lake Elsinore, CA). Journal of Paleolimnology 44, 819-839.
- Kirby, M.E., Feakins, S.J., Bonuso, N., Fantozzi, J.M., Hiner, C.A., 2013. Latest Pleistocene to
- Holocene hydroclimates from Lake Elsinore, California. Quaternary Science Reviews 76, 1-15.
- Kirby, M.E., Poulsen, C.J., Lund, S.P., Patterson, W.P., Reidy, L., Hammond, D.E., 2004. Late
- Holocene lake-level dynamics inferred from magnetic susceptibility and stable oxygen isotope
- data: Lake Elsinore, Southern California (USA). Journal of Paleolimnology 31, 275-293.
- Kirby, M.E., Zimmerman, S.R.H., Patterson, W.P., Rivera, J.J., 2012. A 9170-year record of
- decadal-to-multi-centennial scale pluvial episodes from the coastal Southwest United States: a
- role for atmospheric rivers? Quaternary Science Reviews 46, 57-65.

- Lane, P.N.J., Sheridan, G.J., Noske, P.J., 2006. Changes in sediment loads and discharge from
- small mountain catchments following wildfire in south eastern Australia. Journal of Hydrology
- 702 331, 495-510.
- Larsen, D.J., Miller, G.H., Geirsdóttir, Á., 2013. Asynchronous Little Ice Age glacier
- fluctuations in Iceland and European Alps linked to shifts in subpolar North Atlantic circulation.
- Earth and Planetary Science Letters 380, 52-59.
- Lee, J.-E., Fung, I., 2008. "Amount effect" of water isotopes and quantitative analysis of post
- 707 condensation processes. Hydrological Processes 22, 1-8.
- Loarie, S.R., Carter, B.E., Hayhoe, K., McMahon, S., Moe, R., Knight, C.A., Ackerly, D.D.,
- 709 2008. Climate Change and the Future of California's Endemic Flora. PLoS ONE 3, e2502.
- Macdonald, G.M., Case, R.A., 2005. Variations in the Pacific Decadal Oscillation over the past
- 711 millennium. Geophysical Research Letters 32, doi:10.1029/2005GL022478.
- Makou, M.C., Eglinton, T.I., Oppo, D.W., Hughen, K.A., 2010. Postglacial changes in El Nino
- and La Nina behavior. Geology 38, 43-46.
- Mann, M.E., Zhang, Z., Rutherford, S., Bradley, R.S., Hughes, M.K., Shindell, D., Ammann, C.,
- Faluvegi, G., Ni, F., 2009. Global Signatures and Dynamical Origins of the Little Ice Age and
- 716 Medieval Climate Anomaly. Science 326, 1256-1260.
- 717 McCabe-Glynn, S., Johnson, K.R., Strong, C., Berkelhammer, M., Sinha, A., Cheng, H.,
- 718 Edwards, R.L., 2013. Variable North Pacific influence on drought in southwestern North
- America since AD 854. Nature Geosci 6, 617-621.
- Meko, D.M., Stockton, C.W., Boggess, W.R., 1980. A tree-ring reconstruction of drought in
- southern California. Journal of the American Water Resources Association 16, 594-600.

- Mensing, S., Byrne, R., 1998. Pre-mission invasion of Erodium cicutarium in California. Journal
- 723 of Biogeography 25, 757-762.
- Mensing, S.A., Sharpe, S.E., Tunno, I., Sada, D.W., Thomas, J.M., Starratt, S., Smith, J., 2013.
- The Late Holocene Dry Period: multiproxy evidence for an extended drought between 2800 and
- 1850 cal yr BP across the central Great Basin, USA. Quaternary Science Reviews 78, 266-282.
- Namias, J., Yuan, X., Cayan, D.R., 1988. Persistence of North Pacific Sea Surface Temperature
- and Atmospheric Flow Patterns. Journal of Climate 1, 682-703.
- Neelin, J.D., Langenbrunner, B., Meyerson, J.E., Hall, A., Berg, N., 2013. California Winter
- 730 Precipitation Change under Global Warming in the Coupled Model Intercomparison Project
- 731 Phase 5 Ensemble. Journal of Climate 26, 6238-6256.
- Norris, J., Norris, L., 1994. History of Zaca Lake. The Olive Press Publications, Los Olivos, CA.
- Padilla, M., 2010. Holocene paleoclimate reconstruction using sediments from Overflow Lake,
- 734 Santa Barbara County, California, Department of Geological Sciences. California State
- 735 University, Fullerton, California State University, Fullerton, p. 42.
- Pierce, D.W., Cayan, D.R., Das, T., Maurer, E.P., Miller, N.L., Bao, Y., Kanamitsu, M.,
- Yoshimura, K., Snyder, M.A., Sloan, L.C., Franco, G., Tyree, M., 2013. The Key Role of Heavy
- 738 Precipitation Events in Climate Model Disagreements of Future Annual Precipitation Changes in
- 739 California. Journal of Climate 26, 5879-5896.
- Reimer, P.J., Baillie, M.G.L., Bard, E., Bayliss, A., Beck, J.W., Blackwell, P.G., Ramsey, C.B.,
- Hajdas, R.L., Friedrich, M., Grootes, P.M., Guilderson, T.P., Hajdas, I.,
- Heaton, T.J., Hogg, A.G., Hughen, K.A., Kaiser, K.F., Kromer, B., McCormac, F.G., Manning,
- S.W., Reimer, R.W., Richards, D.A., Southon, J.R., Talamo, S., Turney, C.S.M., van der Plicht,

- J., Weyhenmeye, C.E., 2009. Intcal09 and Marine09 Radiocarbon Age Calibration Curves, 0-
- 745 50,000 Years Cal Bp. Radiocarbon 51, 1111-1150.
- Ren, X., Zhang, Y., Xiang, Y., 2008. Connections between wintertime jet stream variability,
- oceanic surface heating, and transient eddy activity in the North Pacific. Journal of Geophysical
- Research: Atmospheres 113, D21119.
- Reneau, S.L., Katzman, D., Kuyumjian, G.A., Lavine, A., Malmon, D.V., 2007. Sediment
- 750 delivery after a wildfire. Geology 35, 151-154.
- Rodionov, S.N., 2004. A sequential algorithm for testing climate regime shifts. Geophysical
- Research Letters 31, L09204.
- Rubi, L., 2013. Reconstructing late Holocene lake level using littoral cores from Zaca Lake,
- 754 California, Department of Geological Sciences. California State University, Fullerton, California
- 755 State University, Fullerton, p. 34.
- Sachse, D., Billault, I., Bowen, G.J., Chikaraishi, Y., Dawson, T.E., Feakins, S.J., Freeman,
- 757 K.H., Magill, C.R., McInerney, F.A., van der Meer, M.T.J., Polissar, P., Robins, R.J., Sachs, J.P.,
- 758 Schmidt, H.-L., Sessions, A.L., White, J.W.C., West, J.B., Kahmen, A., 2012. Molecular
- 759 Paleohydrology: Interpreting the Hydrogen-Isotopic Composition of Lipid Biomarkers from
- 760 Photosynthesizing Organisms. Annual Review of Earth and Planetary Sciences 40, 221-249.
- Santoso, A., McGregor, S., Jin, F.-F., Cai, W., England, M.H., An, S.-I., McPhaden, M.J.,
- Guilyardi, E., 2013. Late-twentieth-century emergence of the El Nino propagation asymmetry
- and future projections. Nature advance online publication.
- Sarnelle, O., 1992. Contrasting effects of Daphnia on ratios of nitrogen to phosphorus in a
- eutrophic, hard-water lake. Limnology and Oceanography 37, 1527-1542.

- Schimmelmann, A., Lange, C.B., Meggers, B.J., 2003. Palaeoclimatic and archaeological
- evidence for a 200-yr recurrence of floods and droughts linking California, Mesoamerica and
- South America over the past 2000 years. Holocene 13, 763-778.
- Schimmelpfennig, I., Schaefer, J.M., Akçar, N., Ivy-Ochs, S., Finkel, R.C., Schlüchter, C., 2012.
- Holocene glacier culminations in the Western Alps and their hemispheric relevance. Geology.
- Schonher, T., Nicholson, S.E., 1989. The Relationship Between California Rainfall and ENSO
- 772 Events. Journal of Climate 2, 1258-1269.
- Seager, R., Harnik, N., Robinson, W., Kushnir, Y., Ting, M., Huang, H.P., Velez, J., 2005a.
- 774 Mechanisms of ENSO- forcing of hemispherically symmetric precipitation variability. Quarterly
- Journal of the Royal Meteorological Society 131, 1501-1527.
- Seager, R., Kushnir, Y., Herweijer, C., Naik, N., Velez, J., 2005b. Modeling of tropical forcing
- of persistent droughts and pluvials over western North America: 1856–2000. Journal of Climate
- 778 18.
- Seager, R., Ting, M., Li, C., Naik, N., Cook, B., Nakamura, J., Liu, H., 2013. Projections of
- declining surface-water availability for the southwestern United States. Nature Clim. Change 3,
- 781 482-486.
- 782 Stocker, T.F., D. Qin, G.-K. Plattner, L.V. Alexander, S.K. Allen, N.L. Bindoff, F.-M. Bréon,
- J.A. Church, U. Cubasch, S. Emori, P. Forster, P. Friedlingstein, N. Gillett, J.M. Gregory, D.L.
- Hartmann, E. Jansen, B. Kirtman, R. Knutti, K. Krishna Kumar, P. Lemke, J. Marotzke, V.
- 785 Masson-Delmotte, G.A. Meehl, I.I. Mokhov, S. Piao, V. Ramaswamy, D., Randall, M. Rhein, M.
- Rojas, C. Sabine, D. Shindell, L.D. Talley, D.G. Vaughan and S.-P. Xie, 2013. Technical
- 787 Summary. In: Climate Change 2013: The Physical Science Basis. Contribution of Working
- 788 Group I to the Fifth Assessment Report of the Intergovernmental Panel on Climate Change, In:

- 789 Stocker, T.F., D. Qin, G.-K. Plattner, M. Tignor, S.K. Allen, J. Boschung, A. Nauels, Y. Xia, V.
- 790 Bex, P.M. Midgley (Ed.), Cambridge University Press, Cambridge, United Kingdom and New
- 791 York, NY, USA.
- Sun, D., Bloemendal, J., Rea, D., Vandenberghe, J., Jiang, F., An, Z., Su, R., 2002. Grain-size
- 793 distribution function of polymodal sediments in hydraulic and aeolian environments, and
- numerical partitioning of the sedimentary components. Sedimentary Geology 152, 263-277.
- 795 Tanaka, S., Zhu, T., Lund, J., Howitt, R., Jenkins, M., Pulido, M., Tauber, M., Ritzema, R.,
- 796 Ferreira, I., 2006. Climate Warming and Water Management Adaptation for California. Climatic
- 797 Change 76, 361-387.
- Wang, F., Liu, Z., Notaro, M., 2013. Extracting the Dominant SST Modes Impacting North
- 799 America's Observed Climate\*. Journal of Climate 26, 5434-5452.
- Warrick, J.A., Mertes, L.A.K., 2009. Sediment yield from the tectonically active semiarid
- Western Transverse Ranges of California. Geological Society of America Bulletin 121, 1054-
- 802 1070.

809

810

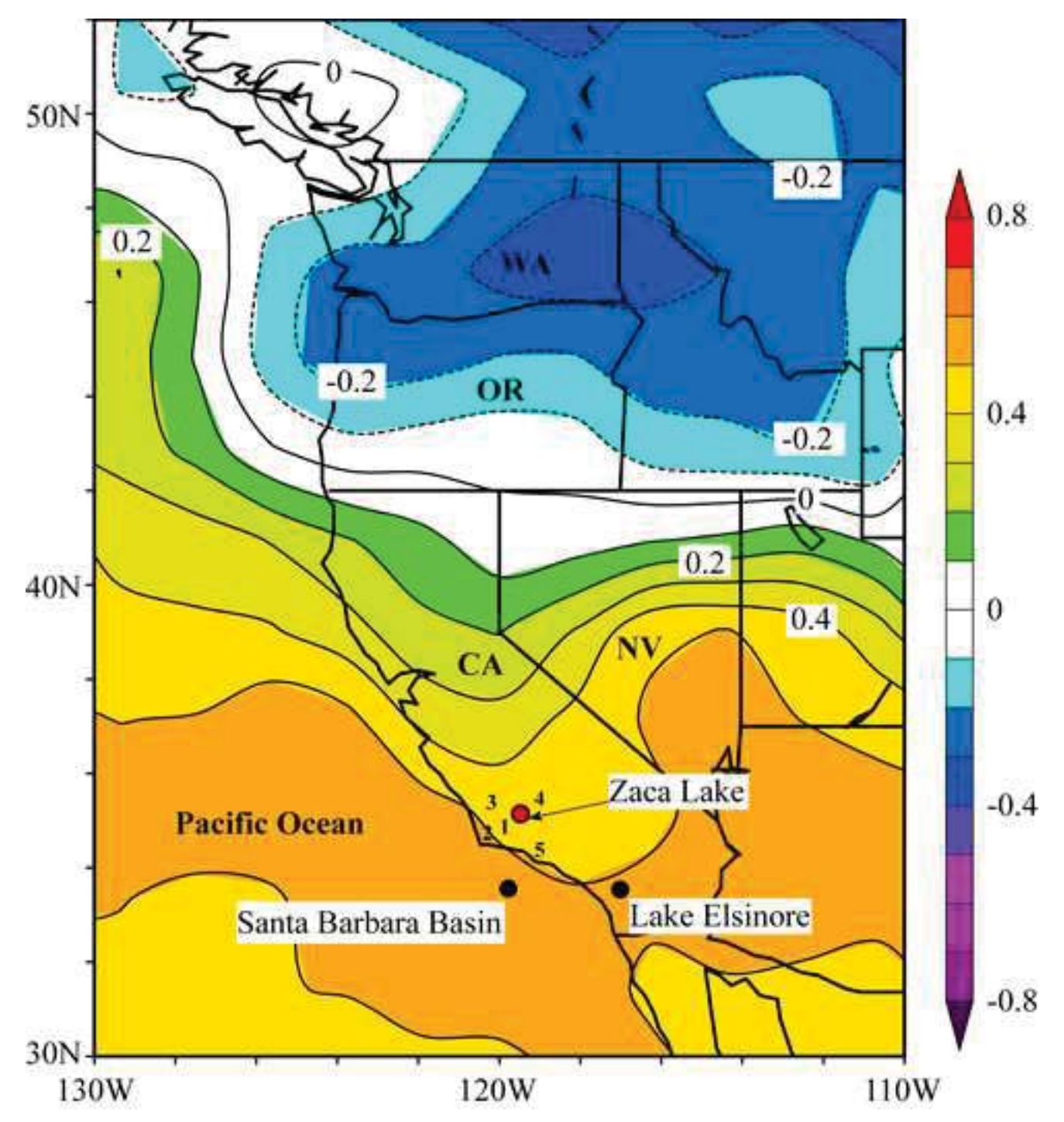
- Williams, A.P., Allen, C.D., Macalady, A.K., Griffin, D., Woodhouse, C.A., Meko, D.M.,
- 804 Swetnam, T.W., Rauscher, S.A., Seager, R., Grissino-Mayer, H.D., Dean, J.S., Cook, E.R.,
- 805 Gangodagamage, C., Cai, M., McDowell, N.G., 2013. Temperature as a potent driver of regional
- forest drought stress and tree mortality. Nature Clim. Change 3, 292-297.
- Yu, J.Y., Kim, S.T., 2013. Identifying the types of major El Niño events since 1870.
- 808 International Journal of Climatology 33, 2105-2112.

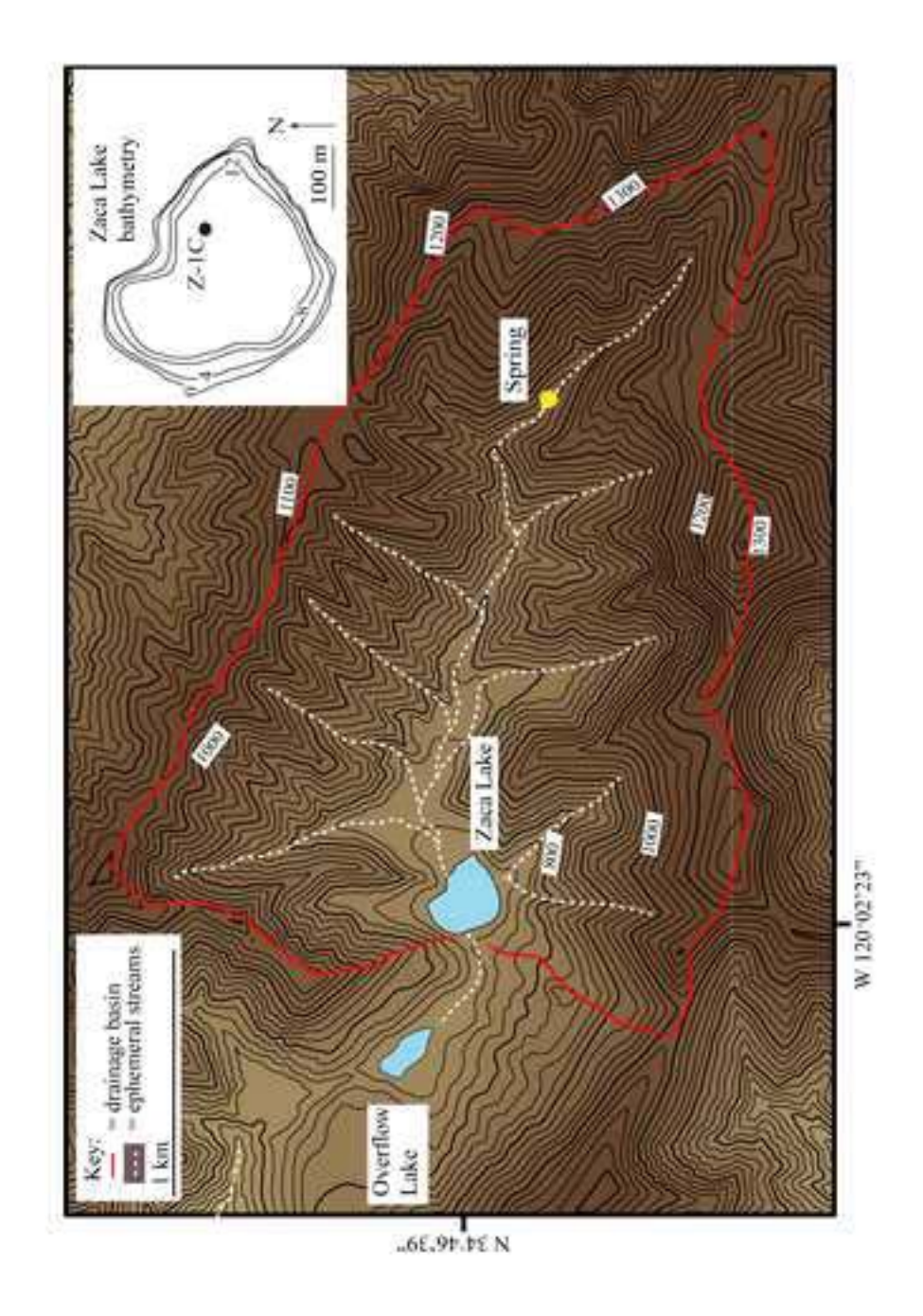
Table 1. Age Data

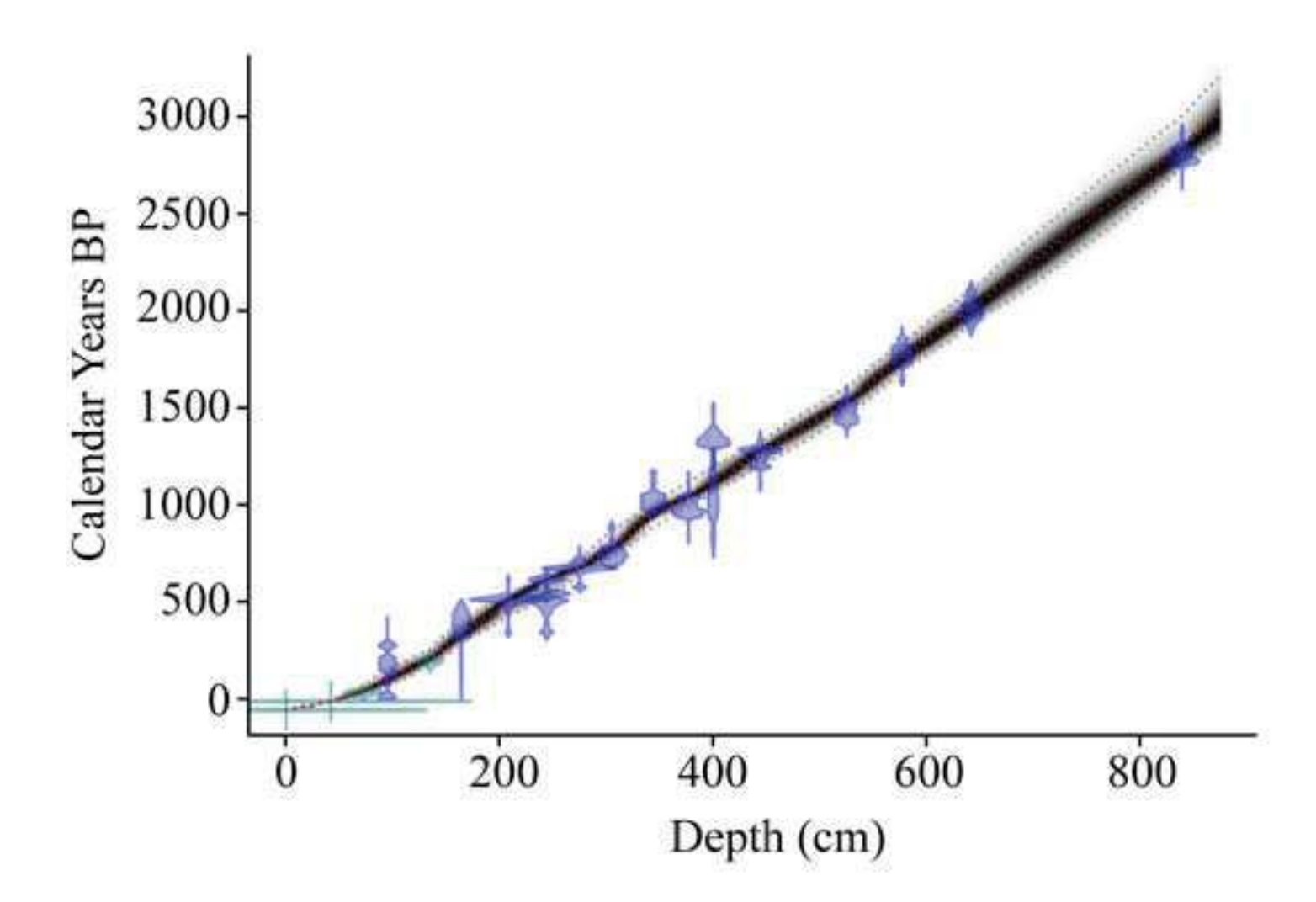
				Mass				$^{14}$ C		cal yr	cal yr	cal yr		
	Depth	Depth CAMS	7.0	of C	$ m d^{13}C$			Year		BP 2s		BP 2s	I	Include
Type	(cm)	#	Notes	(mg)	(0%)	$\mathbf{F}_{\mathbf{mod}}$	Ø	s BP	Ø	min	median	max		þ
Core top	0	n.a.	s/w interface	n.a.	n.a.	n.a.	n.a.	n.a.	0	n.a.	-58	n.a.	*	Yes
Historical	42.5	n.a.	Cs peak	n.a.	n.a.	n.a.	n.a.	n.a.	0	n.a.	-13	n.a.	*	Yes
Pollen	73	n.a.	Eucalyptus FO	n.a.	n.a.	n.a.	n.a.	n.a.	10	n.a.	33	n.a.	*	Yes
$^{14}C$	95.5	144842	2 Twig	1.1	-25	9266.0	0.0039	180	35	0	179	300		Yes
Pollen	135	n.a.		n.a.	n.a.	n.a.	n.a.	n.a.	14	n.a.	193	n.a.	*	Yes
$^{14}C$	164.5		144843 Bark and twigs	0.71	-25	0.9602	0.0041	325	35	305	390	476	*	Yes
$^{14}C$	208.5		144844 Twig and fine organics	1.08	-25	0.9442	0.0034	460	30	484	513	537	*	Yes
$^{14}C$	244.5		147067 Single twig	0.35	-25	0.9332	0.0035	550	30	518	555	638		Yes
$^{14}\mathrm{C}$	244.5		147068 Single twig	0.15	-25	0.9431	0.0046	440	40	331	499	540		Yes
$^{14}$ C	244.5		147070 Stem	0.05	-25	0.5232	0.0070	5210	110	5729	9869	6273		$No^a$
$^{14}\mathrm{C}$	275.5	144845	144845 Twigs	1.01	-25	0.9134	0.0032	725	30	570	675	724	*	Yes
$^{14}\mathrm{C}$	305.5		144846 Twigs, bark, leaf?	0.58	-25	0.9011	0.0031	835	30	889	742	792	*	Yes
$^{14}\mathrm{C}$	344.5		144847 Twig and leaf parts	0.54	-25	0.8703	0.0032	11115	30	938	1018	1171		Yes
$^{14}\mathrm{C}$	377.5		147071 Woody stems, charcoal	0.32	-25.43	0.8740	0.0033	1070	30	929	974	1054	*	Yes
$^{14}\mathrm{C}$	400.5		147072 Woody stems, charcoal	90.0	-25	0.8638	0.0087	1100	06	662	1029	1258	*	Yes
$^{14}\mathrm{C}$	400.5		147073 Mixed organics <1-2mm	0.28	-26.68	0.8340	0.0037	1430	40	1288	1331	1391		Yes
$^{14}\mathrm{C}$	444.5		144848 Rootlets?, grasses?, leaf?	0.20	-25	0.8468	0.0036	1335	35	1183	1273	1306	*	Yes
$^{14}\mathrm{C}$	525.5		144849 Wood	1.16	-25	0.8201	0.0029	1595	30	1410	1474	1548	*	Yes
$^{14}\mathrm{C}$	577.5	14485(	144850 Leaf, grasses	96.0	-25	0.7955	0.0028	1840	30	1708	1776	1864	*	Yes
$^{14}\mathrm{C}$	585.5		147074 Woody stems, mostly charcoal	0.17	-25	0.7431	0.0032	2370	40	2328	2407	2682		$No^a$
$^{14}\mathrm{C}$	642		144851 Seed pods?, very fine organics	0.80	-25	0.7756	0.0027	2040	30	1903	1995	2111	*	Yes
$^{14}C$	778.5		144852 Very fine organic fibers	0.23	-25	0.7888	0.0031	1905	35	1737	1851	1926		$^{ m p}$
$^{14}$ C	800.5	144853	3 Delicate twigs and bark	0.41	-25	0.7887	0.0029	1905	30	1739	1852	1925		$No^{b}$
$^{14}$ C	806.5		144854 Delicate charcoal and small twigs	0.18	-25	0.7885	0.0033	1910	35	1737	1857	1931		No
$^{14}C$	839.5	147076	147076 Woody stems, mostly charcoal	0.13	-25	0.7152	0.0034	2680	40	2747	2788	2854	*	Yes
C 1.	1.1	1 - 4 + 1- I	(ODI)	n 11	1 . 1	7 1 1 7 7 1				Dollan o	11/	D -: 1	(117	

1994a) and estimated maturity. FO = first occurrence. CAMS# = sample identification number from measurements at the Lawrence Livermore National Laboratory Berkeley) are assigned dates based on first appearance (Mensing and Byrne 1998) of Erodium (1755-1760), Eucalyptus based on planting date (Norris and Norris, measured by D. Hammond at the University of Southern California (USC). Pollen = historical dates from invasive species. Pollen counts (by L. Reidy at UC (LLNL). F<sub>mod</sub> = Fraction modern. cal = calibrated age using Intcal13 (Reimer et al., 2013). \* Published in Feakins et al., (2014). Included in this age model: <sup>a</sup>excluded by Bayesian approach; <sup>b</sup> excluded by authors see text.

\*Figure1
Click here to download high resolution image







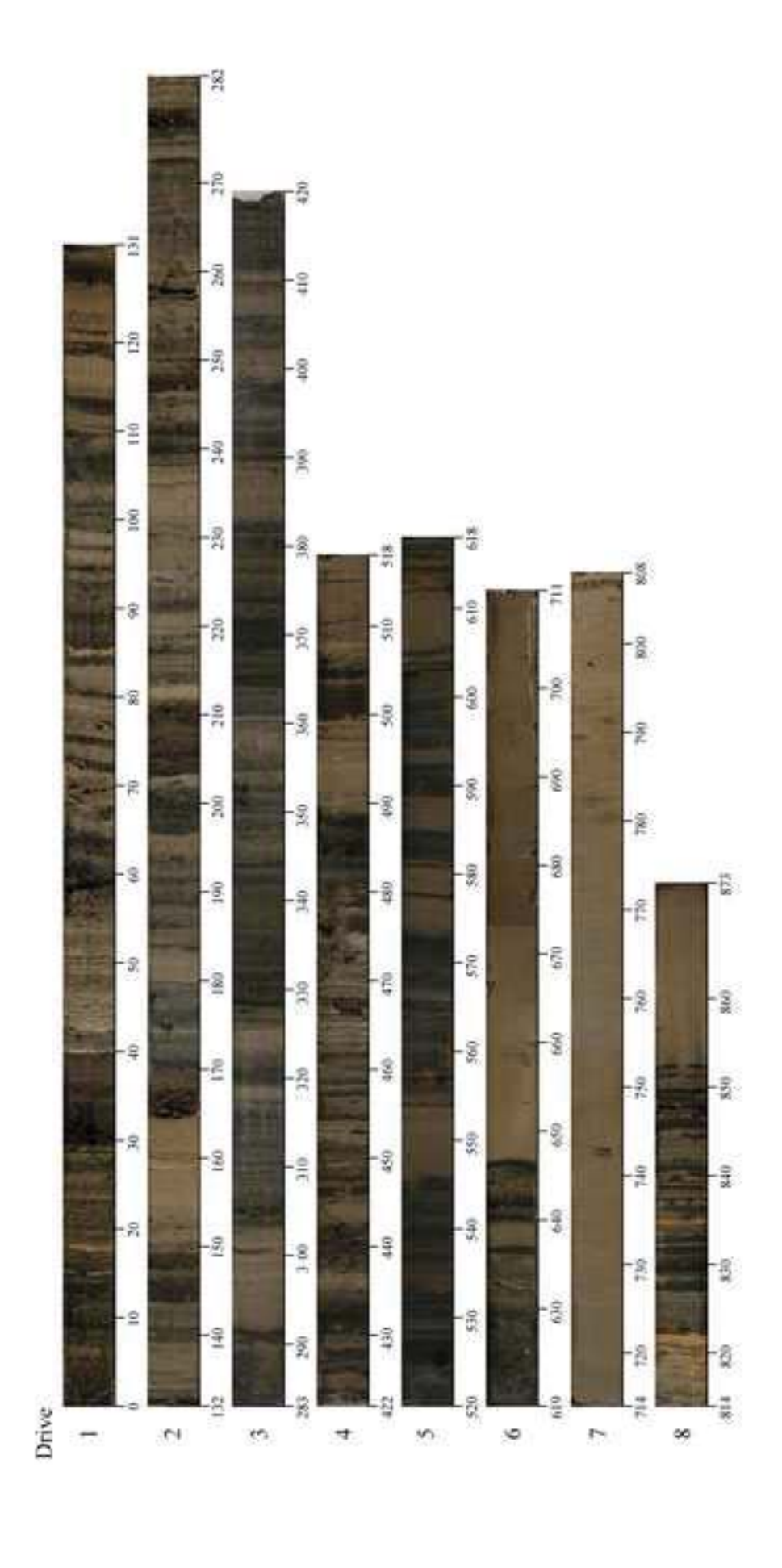


Figure 4

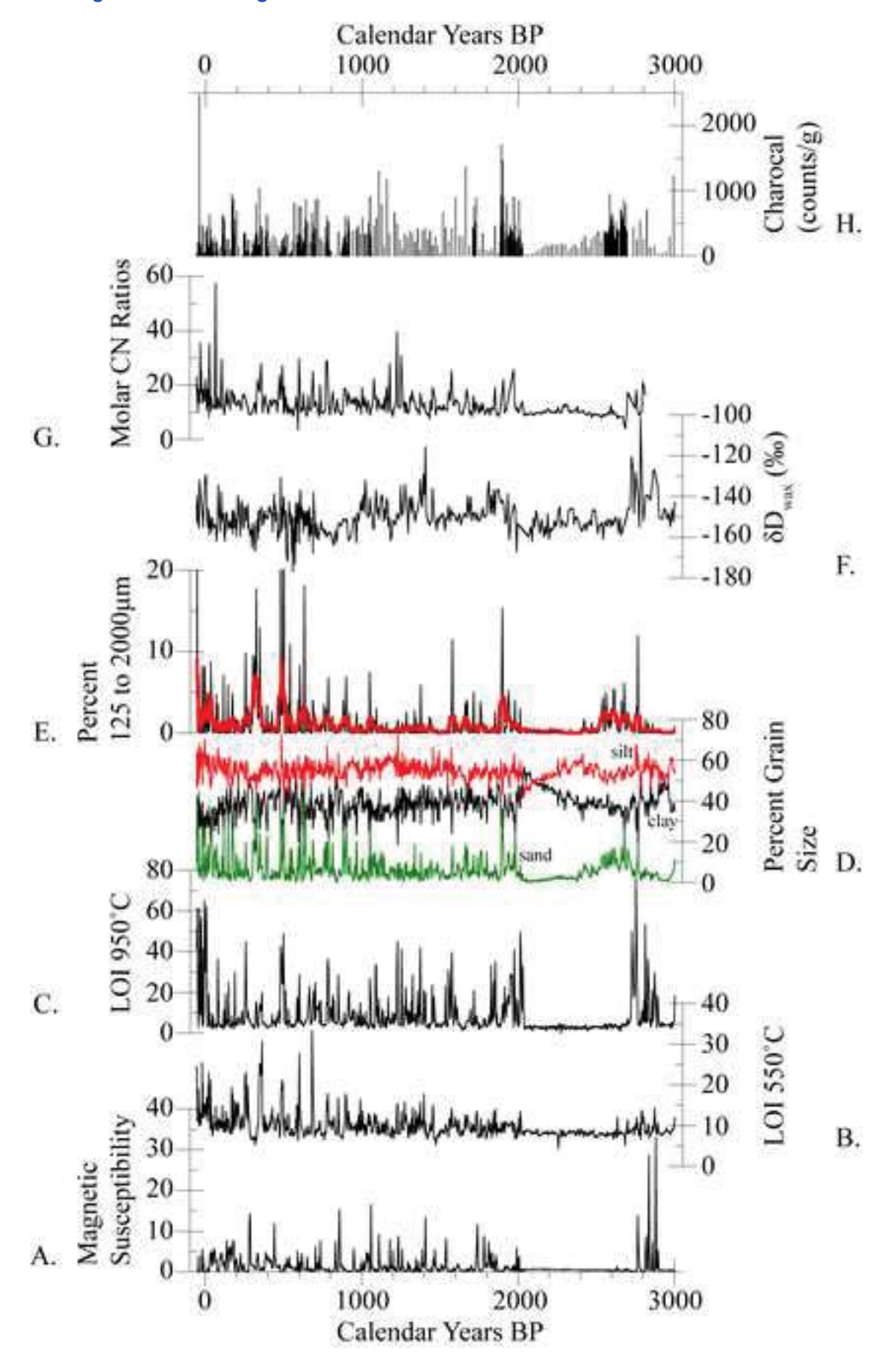


Figure 5

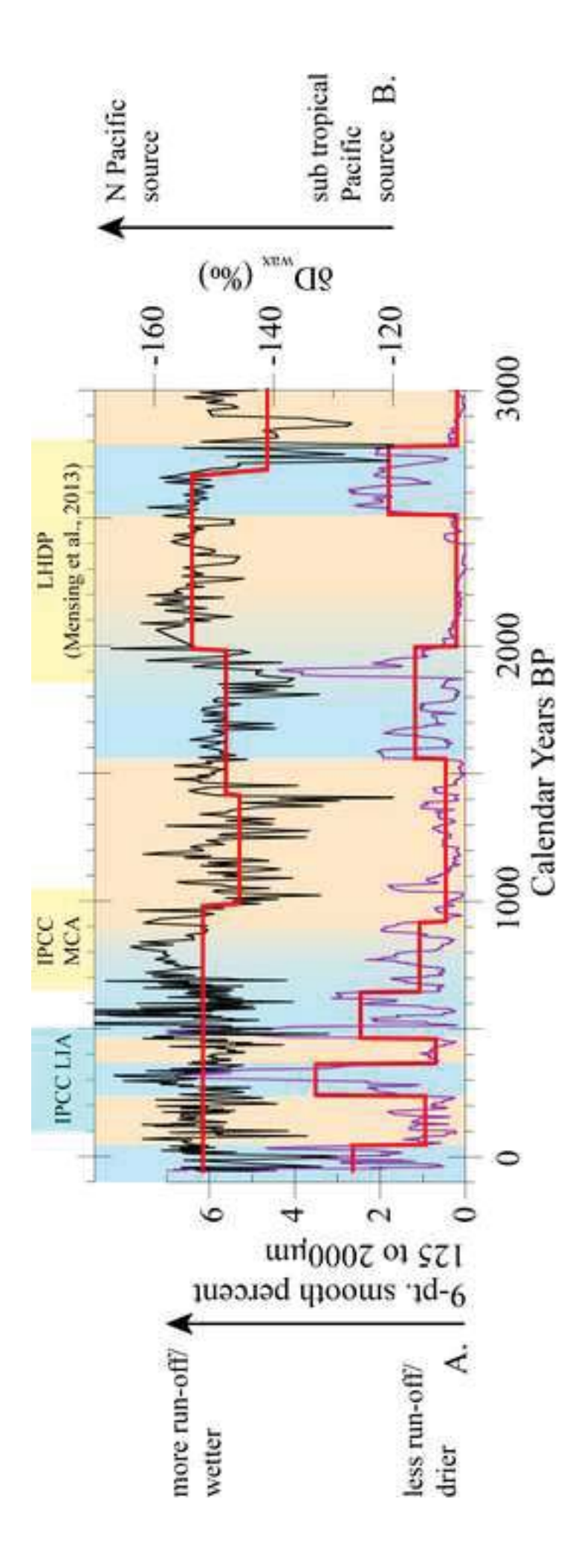


Figure 6

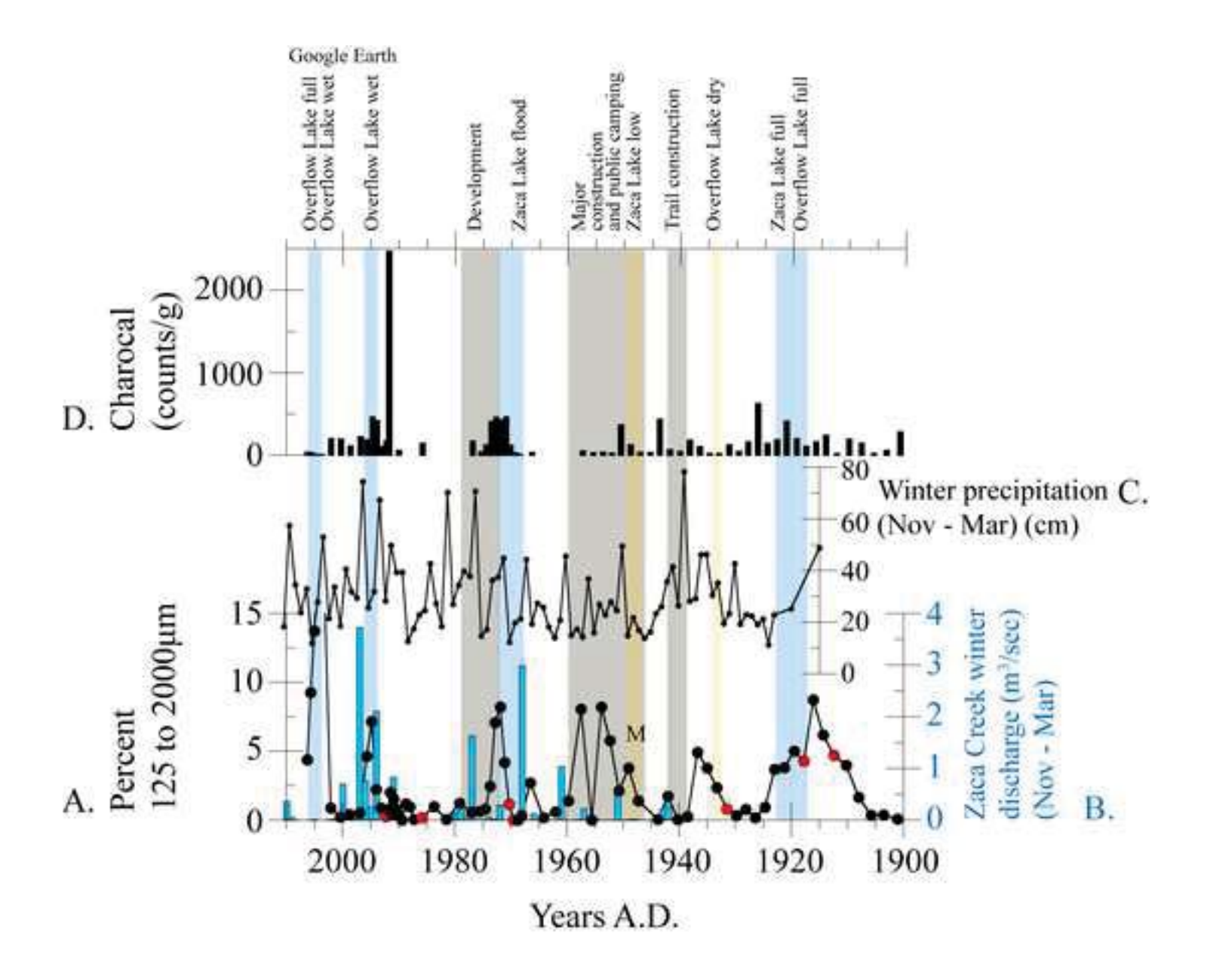


Figure 7

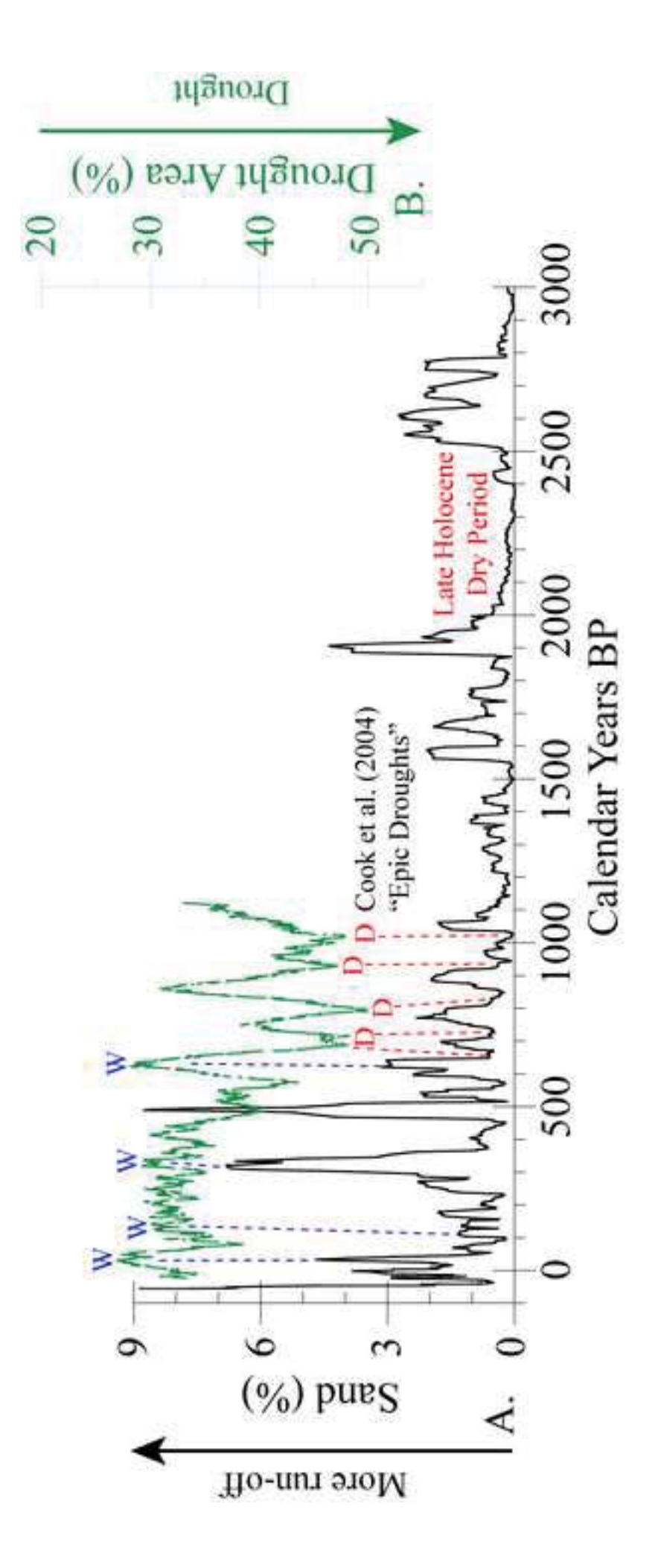


Figure 8

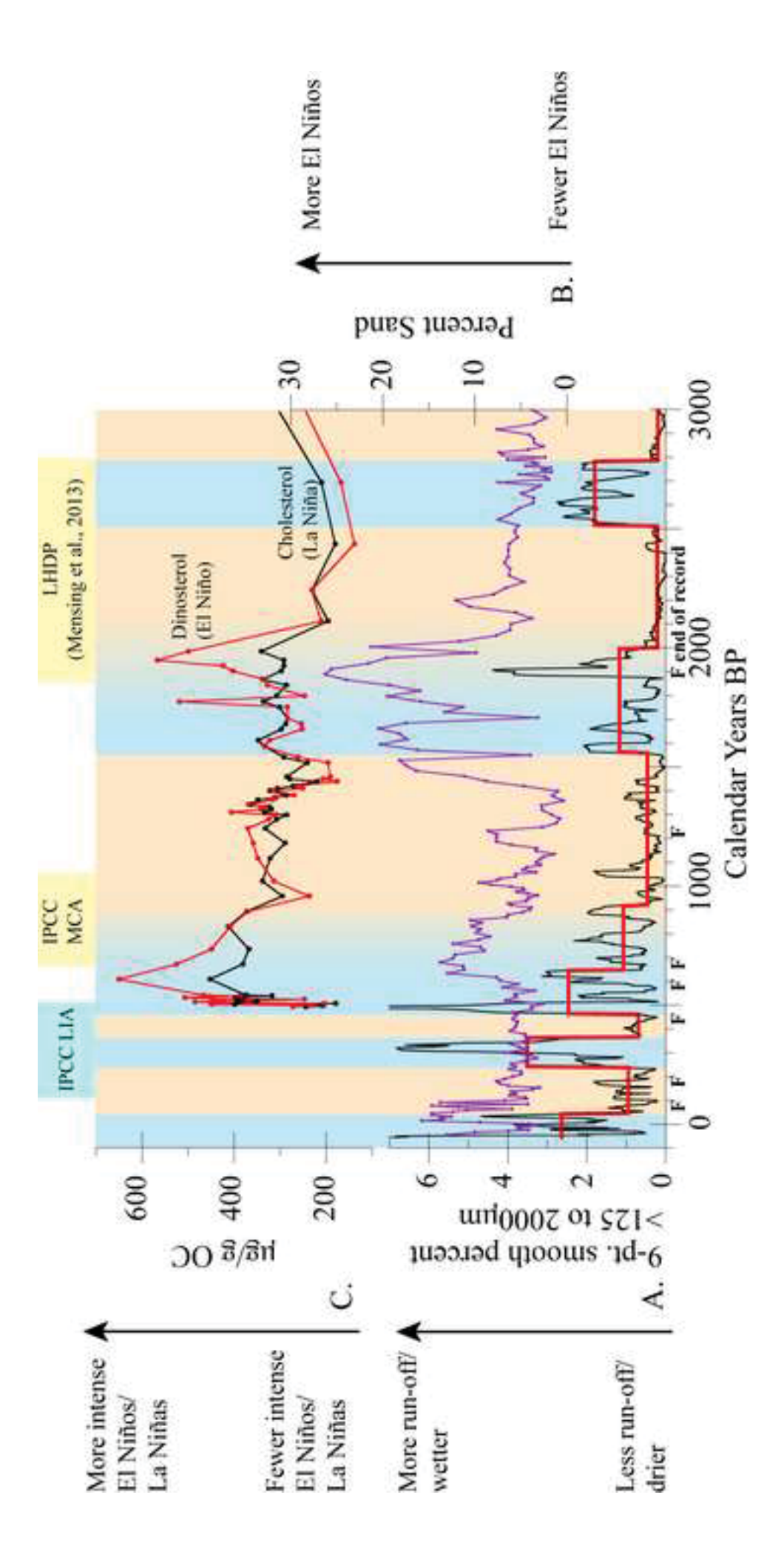


Figure 9